Deterministic and Stochastic Sensitivity Analysis of a Mathematical Model for Polymer Flooding

by

Hans Petter Langtangen

Deterministic and Stochastic Sensitivity Analysis of a Mathematical Model for Polymer Flooding

Hans Petter Langtangen*

October 1989

Abstract

The sensitivity of the solution of the equations governing one–dimensional polymer flooding in an oil reservoir is investigated with respect to uncertainties in the input parameters, such as porosity, absolute and relative permeabilities, and adsorption functions. In the standard deterministic model perturbations in the time to water breakthrough in the production well, due to controlled perturbations in the input data, are reported. It is found that the sensitivity is significant. A corresponding stochastic flow model is analyzed by tools from structural reliability theory. Sensitivity measures of the statistics of the time to breakthrough are reported. Correlations between the input variables seem to have a considerable effect on their relative importance.

*Department of Mathematics, University of Oslo, P. O. Box 1053, N–0316 Oslo 3, Norway.

Contents

1 Introduction

The rapid growth of computer power and efficient numerical methods has made it possible to solve very complex mathematical models. In many areas, and particularly in multi–phase reservoir flow mechanics, the mathematical models contain physical assumptions and input data which are subjected to rather large uncertainties. Surprisingly, systematic investigations of such uncertainties in reservoir models seem to have attracted little attention in the literature compared to development of more sophisticated mathematical models and numerical solution schemes.

Most of the literature on input parameter uncertainties and heterogeneities in reservoir flow discuss deterministic methods for obtaining representative "mean" values of the rock parameters ([3], [9], [16]), given some random variation of these parameters. Specific values of the input parameters are also often determined by (incomplete) solution of inverse problems, e.g. as in history matching. In such an approach the output of the code is compared to some physical observations and the input parameters are adjusted iteratively to obtain a procedure where (hopefully) the output values converge to the observed values. A serious problem with this approach is that the available physical observations are so limited that the inverse problem becomes under determined. The computed input parameters therefore represent one out of an infinite number of possible solutions.

Recently, statistical methods have begun to attract some attention in reservoir simulation, see e.g. [15] or [6]. It is expected that stochastic reservoir simulation will become commercially available during the next decade, but presently the long CPU time associated with such approaches is prohibitive. Also in a stochastic simulator there will be input data to the code that are subjected to uncertainties. However, the stochastic approach can in a particular flow problem to a larger extent than a deterministic model utilize information inherent in experimental data and engineering experience.

By the term deterministic sensitivity analysis we shall mean investigation of the sensitivity to input data in a deterministic simulator. Consequently, stochastic sensitivity analysis refers to sensitivity study of a stochastic reservoir simulator.

The aim of the first part of this note is to investigate the sensitivity of an important output parameter from a deterministic reservoir simulator to controlled perturbations in the input data. Besides ranking of the input parameters according to their relative importance we also give exact numerical estimates of the input/output perturbations. As the number of simulations required in such a study becomes very large, only a one–dimensional flow model has been employed for the investigations herein. It is also natural to gain insight into the sensitivities of the one–dimensional problem before investigating more complicated two– and three–dimensional flow cases. The governing equations are solved numerically and model a two–phase EOR polymer flooding process without capillary effects. The

output parameter is chosen as the time to water breakthrough in the production well. This quantity is also closely related to the total oil production until water breakthrough. We are especially interested in the sensitivity to parameters that must be measured from laboratory experiments on core samples, such as porosity, absolute permeability, relative permeabilities and adsorption functions. Since only experimental data from the rock near the wells are available, it is important to introduce space variation of the input parameters between the wells. Special emphasis is here paid to heterogeneous media and the influence of an assumed piecewise linear or discontinuous variation of the rock parameters.

In a deterministic sensitivity analysis there are two main approaches. The first and most obvious idea is to perturb one input parameter and measure the corresponding perturbation in the output parameter by solving the governing equations. This approach is mainly used here, and it is previously employed in reservoir flow by Evrenos and Comer [7] in a sensitivity study of gas–water relative capillarity and permeability. However, in comparison with [7] our investigation involves much more numerical experiments, a different mathematical model, and a different organization of the analysis. The second technique utilize linear partial differential equations for sensitivity coefficients ([17]). This may be a very effective approach if integrated in implicit (nonlinear) solution algorithms. We present some examples showing that this latter technique is inapplicable in reservoir flow where the solutions frequently contain shocks.

The goal of deterministic sensitivity analysis is twofold. Firstly, it is to determine the ranking of the input parameters according to their relative influence on output perturbation. This ranking will point out the input parameters which are most important to measure accurately and will also provide insight into the mechanics of the flow model. Secondly, the sensitivity analysis give information about the accuracy of the output given a (commonly accepted) inaccuracy in the input data. This level of accuracy is of particular interest e.g. when a mathematical model is integrated in a comprehensive project context, also including social and economic factors.

In a stochastic reservoir simulator the uncertainty of the input parameters of the deterministic mathematical model are expressed by a joint probability distribution. However, in practice it is difficult to establish more than marginal distributions for each parameter and maybe some correlation coefficients. Variants of Monte–Carlo simulation techniques are presently dominating in stochastic reservoir simulation ([6]). A large number of input parameter sets are generated in accordance with the prescribed statistical distribution of the parameters. Then the flow model is solved for each parameter set and a statistical analysis of the output results is performed. Another, more analytical, approach utilize recent results from structural reliability theory. We show that this latter type of method

is well suited for the problems treated in this note, and therefore adopt these in the stochastic sensitivity analysis. A technical report by Selvig [15] is, to this author's knowledge, the only attempt to apply structural reliability methods to reservoir flow mechanics. Some activity on applications of such reliability methods to finite element discretized continua is emerging ([12]), but up to now structural reliability methods have mostly been applied to compute the failure probability of static beam structures under different loading conditions. A general discussion of Monte–Carlo simulation and analytically based reliability methods are given by Bjerager [4].

In the stochastic sensitivity analysis we may have three aims. The first is to measure the sensitivity to the input data in a stochastic reservoir simulator. Such data includes quantities that describe the statistical distributions as well as ordinary deterministic parameters entering the problem. This type of sensitivity measure is closely related to that used for the deterministic simulator, but the nature of the two types of analysis makes it natural to present the results slightly differently. Our second goal is to rank the most important stochastic variables in the flow problem. This yields information on which input parameters that need to be modeled stochastically. The final aim would be to relate uncertainty in input, for example in terms of standard deviations, to uncertainty in output. However, this requires a complete probability distribution of the output parameter. Although it is possible to calculate such distributions with the present methods of stochastic analysis, the amount of computational work has been considered to large in this initial study.

We remark that a quantitative comparison of deterministic and stochastic sensitivity analysis is impossible, due to the different nature of a deterministic and a stochastic simulator. However, qualitative comparison may be of interest, especially to increase the understanding of the impact of different input data on the final output of the simulator.

Although the present note concerns the particular problem of oil reservoir flow, the proposed approach is of a general character. Similar investigations should be of interest in other fields where the mathematical models require input data subjected to significant uncertainties.

2   The governing equations

Polymer flooding is an enhanced oil recovery (EOR) technique where a mixture of water and a polymer is injected in the reservoir to displace oil. The appearance of the polymer causes the viscosity ratio between the injected and displaced fluid phases to decrease and thereby enhance the recovery process (see [8]).

We consider the flow of two immiscible, incompressible phases, one aqueous

phase and one oil phase, in a porous medium. Only space variations in one direction is taken into account. The aqueous phase consists of water and a polymer component, which is totally miscible in water. Let S be the saturation of the aqueous phase (i.e. $1 - S$ is the oil saturation), and let C be the concentration (mass fraction) of the polymer component in the aqueous phase (clearly, $1 - C$ is the concentration of water in the aqueous phase). By applying Darcy's law, the principle of mass conservation, and neglecting capillary pressure effects one may derive the following system of partial differential equations governing S and C for $0 < x < L$ and $t > 0$:

$$\phi\frac{\partial S}{\partial t} + v\frac{\partial F}{\partial x} = 0, \tag{1}$$

$$\phi\frac{\partial}{\partial t}[SC + A] + v\frac{\partial}{\partial x}[CF] = 0. \tag{2}$$

where x is the space coordinate, t denotes time, v is the total Darcy filtration velocity (independent of x), and ϕ is the porosity. F is the fractional flow function ([14]) which depends on S and C. Adsorption of the polymer on the rock is modeled by the function A that depends on C. The above two equations determine S and C when v is known. This is the case if the injection velocity is controlled in the injection well ($x = 0$). If instead the pressure difference between the injection and production well is prescribed, v will depend on the pressure field P which is governed by

$$\frac{\partial}{\partial x}\left(H\frac{\partial P}{\partial x}\right) = 0. \tag{3}$$

We have $v = -H\partial P/\partial x$, where H is a function of S and C. In this latter case v will be a function of time. In mathematical literature on one–dimensional polymer flooding it is common to treat v as a known constant. However, this may result in a peculiar fact: If v is prescribed in one–dimensional flow then the absolute permeability only enters the equations (1) and (2) through the gravity terms, and the effect of the absolute permeability is small. On the contrary, when the pressure difference is prescribed, the velocity v is approximately proportional to the absolute permeability, with the consequence that the output quantities become highly sensitive to the value of the absolute permeability, which is always the case in two– and three–dimensional flow. In this work we therefore employ pressure boundary conditions that result in a realistic influence of the absolute permeability.

The fractional flow function has the form

$$F = \frac{k_{rw}}{k_{rw} + \mu k_{ro}} \tag{4}$$

where k_{rw} and k_{ro} are the relative permeability of the aqueous and oil phases, respectively. Here $\mu = \mu_a/\mu_o$, where μ_a and μ_o are the viscosities of the aqueous and oil phases, respectively. We have not included gravity effects in this paper.

We have nevertheless studied these effects and found them less interesting in a sensitivity analysis context. The viscosity of the aqueous phase depends on the polymer concentrations. In this work we have employed a linear relation between μ_a/μ_o and the concentration C:

$$\mu = \nu + \zeta \cdot 100C.$$

If $C = 0$ then $\nu = \mu_w/\mu_o$, where μ_w is the water viscosity. We may typically have $1 \leq \zeta \leq 2$. The relative permeability curves have been written on the form

$$k_{rw}(S) \;=\; K_{wm} \left[\frac{S - S_{wr}}{1 - S_{or} - S_{wr}} \right]^a \tag{5}$$

$$k_{ro}(S) \;=\; K_{om} \left[\frac{1 - S - S_{or}}{1 - S_{wr} - S_{or}} \right]^b \tag{6}$$

Here K_{wm} and K_{om} are maximum values of k_{rw} and k_{ro}, respectively, S_{wr} is the irreducible saturation of the aqueous phase, and S_{or} is the irreducible oil saturation. Figure 1 shows the geometric interpretation of the parameters in the relative permeability curves. The function H, which enters the pressure equation (3), has the form

$$H = \hat{K} \left(\frac{k_{rw}}{\mu_a} + \frac{k_{ro}}{\mu_o} \right).$$

Here $\hat{K}$ is the absolute permeability. However, it is convenient to define a characteristic absolute permeability κ, and introduce $K = \hat{K}/\kappa$. This K will in the rest of the paper be referred to as the absolute permeability. The adsorption function is assumed to have the form

$$A = \frac{\xi \cdot 100C}{1 + \eta \cdot 100C},$$

where ξ and η are empirically determined constants.

The parameters introduced above must fulfill the following constraints:

$$S_{wr} \leq S \leq 1 - S_{or}$$
$$0 \leq S_{wr} + S_{or} \leq 1$$
$$0 \leq C \leq 1$$
$$0 \leq K_{wm} \leq 1$$
$$0 \leq K_{om} \leq 1$$
$$a, b, K, \mu > 0$$
$$0 < \phi < 1$$
$$\xi, \eta \geq 0$$

As initial and boundary conditions for the equations (1), (2) and (3) we have used:

$$S(x, 0) \;=\; S_{wr}$$

$$S(0,t) = 1 - S_{or}^0$$
$$C(x,0) = 0$$
$$C(0,t) = \begin{cases} \Lambda & t < t_s \\ 0 & t \geq t_s \end{cases}$$
$$P(0,t) = \Delta P$$
$$P(L,t) = 0$$

where S_{or}^0 denotes S_{or} at $x = 0$. Recall that only pressure differences, and not the pressure level, influence incompressible flow. The injection concentration Λ is usually small, typically $\Lambda = 0.01$. With these boundary and initial conditions the typical qualitative features of the solution in a homogeneous medium are:

- There is one shock in C, say at $x = x_s$. C equals the constant Λ behind the shock, provided $t_s > t$. For $t_s < t$, the C profile becomes plug formed.

- When adsorption is present, there are two shocks in S, one at $x = x_s$ and one for $x > x_s$. The two shocks reduce to one single when $A \to 0$.

Observe that the well-known Buckley-Leverett problem ([14]) is a special case of the polymer model where either C is constant or $\zeta = 0$.

A central finite difference method is used for solving the elliptic pressure equation (3). The two hyperbolic conservation laws (1) and (2) are solved by the
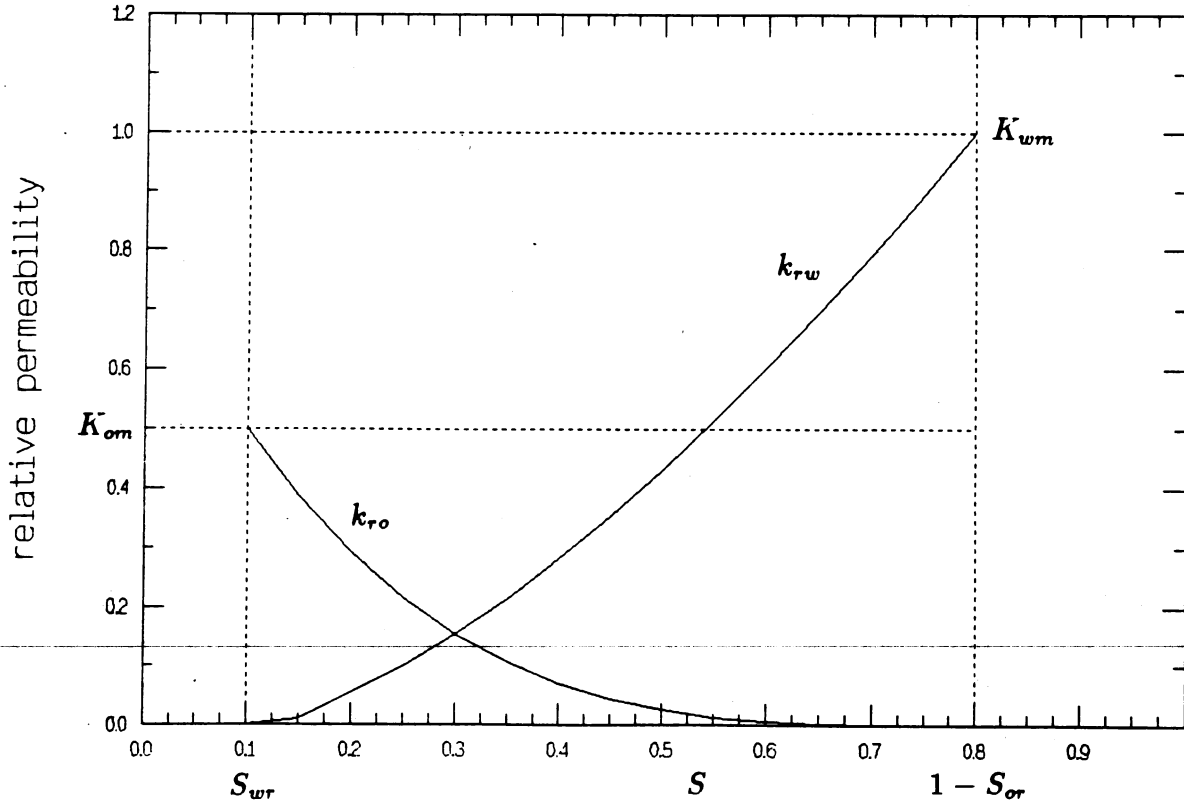

Figure 1: *Example of parameters entering the relative permeability curves.* $a = 1.5$, $b = 3.5$, $S_{wr} = 0.1$, $S_{or} = 0.2$, $K_{wm} = 1.0$, $K_{om} = 0.5$.

explicit first-order Godunov (upwind) scheme on a uniformly partioned grid with N grid points ([10]). Let Δt be the time step length and let Δx be the spacing in the grid. The stability requirement can be deduced from Johansen *et al.* [10] and is in our case

$$\Delta t \leq \Delta x \min_{0 \leq x \leq L} \left(\frac{\phi}{v \left| \frac{\partial F}{\partial S} \right|}, \frac{\phi}{v \xi} \right).$$

In each simulation we have chosen Δt as large as possible according to this stability criterion.

The present numerical scheme leads to rather diffusive solution for C, and the C shock usually extends over 8–10 intervals. If there is only a single shock in S, our scheme resolves this shock quite satisfactorily, that is, over about two grid intervals. When there are two shocks in S, the shock which has the same position as the shock in C is dispersed over 8–10 intervals (due to the diffusive C profile). The shock in the front of the saturation profile is ordinarily resolved over a couple of grid intervals.

3 Deterministic analysis

3.1 Sensitivity measures

Let $\mathbf{p} = (p^1, \ldots, p^q)^T$ be a vector of space varying, empirically determined, parameters entering the governing equations (1) and (2). Heterogeneity modeling will require that $\mathbf{p}$ is defined for each of the N points in the computational mesh. Since the basic equations may develop shock solutions, N is usually large, and it is not possible in practice to accurately determine $\mathbf{p}$ at each point. Therefore we suggest to introduce a coarse "parameter grid". Suppose we want $\mathbf{p}$ to be piecewise linear. Then we may define a parameter grid $(y_0, \ldots, y_M)$ where $M << N$, $y_0 = 0$ and $y_M = L$. The vector $\mathbf{p}$ is then defined only for each y_i, $i = 0, \ldots, M$, and we let $\mathbf{p}_i = (p_i^1, \ldots, p_i^q)^T$ denote the value of $\mathbf{p}$ at $x = y_i$. Intermediate values of $\mathbf{p}$ in an interval $[y_i, y_{i+1}]$ are computed by linear interpolation. The space variation of rock properties is often discontinuous. This can be modeled by partitioning $\Omega = [0, L]$ into $M + 1$ non-overlapping intervals Ω_i, $i = 0, \ldots, M$. On each Ω_i, $\mathbf{p}$ is constant in space and the value is denoted by $\mathbf{p}_i$. For each i and j we constrain the perturbed values p_i^j to lie in the interval I_i^j.

To measure the influence of a perturbation in $\mathbf{p}$, we must decide on which output quantities to examine. In this note we have used time to water breakthrough T in the production well, which for the present system of hyperbolic equations and boundary conditions can be defined as

$$T = \inf\{t : S(L, t) > S(L, 0)\}$$

Another interesting quantity is the total volume of oil produced until water break-through:

$$R = \int_0^L \phi[1 - S(x,0)]dx - \int_0^L \phi[1 - S(x,T)]dx$$

$$= \int_0^L \phi S(x,0)dx - \int_0^L \phi S(x,T)dx.$$

Integrating (1) from $x = 0$ to $x = L$ and in time from $t = 0$ to $t = T$ we get

$$R = -\int_0^T v\left[F_{x=L} - F_{x=0}\right] dt$$

From the formulas for the fractional flow function and our boundary and initial conditions it is easily deduced that $F_{x=L} = 0$ for $t < T$ and $F_{x=0} = 1$ for $t > 0$. Therefore

$$R = \bar{v}T$$

where $\bar{v}$ is the time average of v in the time interval $[0,T]$. (Notice that when v is constant in time, (1) implies $T \sim 1/v$ so that R becomes independent of v.)

The sensitivity analysis is organized in the following way. Reference parameter vectors, p_i^{ref}, $i = 0, \ldots, M$, are defined. The value of T obtained with the reference parameter vectors as input is denoted T^{ref}. Then for some $0 \le i \le M$ and $j = 0, \ldots, q$ the parameter p_i^j is perturbed inside the interval I_i^j. The corresponding extreme values of T are denoted $\max T_i^j$ and $\min T_i^j$. T is usually a monotonic function of p_i^j so these extreme values occur at the end points of the intervals I_i^j. Instead of reporting the numbers $\max T_i^j$ and $\min T_i^j$ we report *maximum relative reduction* (MRR)

$$\frac{\min T_i^j - T^{\text{ref}}}{T^{\text{ref}}}$$

and *maximum relative increase* (MRI)

$$\frac{\max T_i^j - T^{\text{ref}}}{T^{\text{ref}}}.$$

For example, MRR measures the maximum relative reduction in the time to break-through when *one* parameter at one coarse mesh grid point is perturbed (inside a specified interval) while *all other* parameters equal the reference values.

We have also calculated T values corresponding to "worst case" (T^{worst}) and "best case" (T^{best}). T^{worst} is computed by choosing $p_i^j \in I_i^j$ (all i and j) so that T is minimized. Similarly, T^{best} corresponds to the choice of all $p_i^j \in I_i^j$ so that T is maximized. We will report AMRR (absolute maximum relative reduction) and AMRI (absolute maximum relative increase) by relating T^{worst} and T^{best} to the reduction/increase in T^{ref} as explained for MRR and MRI above. For example, the AMRI value represents the increase in T^{ref} when *all* input parameters are adjusted (within their intervals) so that T is maximized.

Of the parameters entering the fractional flow function it is physically reasonable to assume that ν and ζ can be treated as known constants without uncertainty. On the contrary, ϕ, K_{wm}, K_{om}, S_{wr}, S_{or}, a, b, K, ξ and η may vary with the space coordinates and must be determined by laboratory experiments on core samples from the wells. One difficulty is to assign a space variation to these parameters between the well values. For sensitivity analysis we introduce the vector $\mathbf{p} = (p^1, \ldots, p^q)^T$, $q = 10$, as

$$p^1 = \phi, \ p^2 = a, \ p^3 = b, \ p^4 = S_{wr}, \ p^5 = S_{or},$$

$$p^6 = K_{wm}, \ p^7 = K_{om}, \ p^8 = K, \ p^9 = \xi, \ p^{10} = \eta.$$

It is advantageous to consider 4 groups of uncertain parameters: (ϕ), (K), $(a, b, S_{wr}, S_{or}, K_{wm}, K_{om})$, and (ξ, η), corresponding to porosity, absolute permeability, fractional flow function (relative permeability) parameters and adsorption function parameters. We define AMRI-F to be the absolute maximum relative increase in T when all fraction flow function parameters $(a, b, S_{wr}, S_{or}, K_{wm}, K_{om})$ are adjusted inside their intervals I_i^j so that T is maximized. Similarly, we define AMRI-A to be the corresponding maximum when the adsorption function parameters are adjusted optimally. The definition of the minimum quantities AMRR-F and AMRR-A should follow directly.

3.2 Solution of equations for sensitivity coefficients

The purpose of sensitivity analysis is to examine the change of an output parameter due to a change $\Delta\mathbf{p}$ in $\mathbf{p}$. To explicitly indicate the dependence of e.g. S upon $\mathbf{p}$, we write $S(x, t; \mathbf{p})$. In this section we examine an approach for obtaining information about $S(x, t; \mathbf{p} + \Delta\mathbf{p})$ which requires solution of the governing equations with $\mathbf{p}$ as input in addition to some *linear* partial differential equations for the *sensitivity coefficients*. For simplicity we restrict the following discussion to the Buckley-Leverett problem, that is, no polymer is present, and the governing equation consist of (1) where F is a function of S only. We also treat v as a given constant, i.e. the pressure equation (3) is not solved.

We define the sensitivity coefficient u_i as

$$u_i(x, t; \mathbf{p}) = \frac{\partial}{\partial p^i} S(x, t; \mathbf{p}), \quad i = 1, \ldots, q. \tag{7}$$

An equation for u_i can be derived by derivation of (1) with respect to p^i. This gives

$$\frac{\partial u_i}{\partial t} + \frac{v}{\phi} \frac{\partial}{\partial x} \left[\frac{\partial F}{\partial S} u_i \right] = -\frac{v}{\phi} \frac{\partial}{\partial x} \left(\frac{\partial F}{\partial p^i} \right) - \frac{\partial}{\partial p^i} \left(\frac{v}{\phi} \right) \frac{\partial F}{\partial x}. \tag{8}$$

Note that $\partial F / \partial p^i$ is carried out by keeping S constant. This equation is linear in u_i since $S(x, t; \mathbf{p})$ is known from equation (1). Observe that the coefficients and

the nonhomogeneous term in the equation for u_i are discontinuous in both space and time. An estimate of $S(x,t; \mathbf{p} + \Delta \mathbf{p})$ can then be calculated from a first–order truncated Taylor series:

$$S(x,t; \mathbf{p} + \Delta \mathbf{p}) \approx S^+(x,t; \mathbf{p}, \Delta \mathbf{p}) \equiv S(x,t; \mathbf{p}) + \sum_{j=1}^{q} u_j(x,t; \mathbf{p}) \Delta p^j. \qquad (9)$$

The use of sensitivity coefficient equations in elliptic groundwater flow has been examined by Yukler [17]. Scalar hyperbolic conservation laws in one space dimension are most conveniently solved by explicit finite difference schemes. In this case the calculation of $S(x,t; \mathbf{p} + \Delta \mathbf{p})$ by the approximate procedure (8) and (9) is computationally more expensive than solving the exact equation (1) with $\mathbf{p} + \Delta \mathbf{p}$ as input. However, in more complex situations where implicit time schemes with Newton-type iterations are used, the solution of a linear equation for a u_i is much cheaper than than solving a nonlinear equation for $S(x,t; \mathbf{p} + \Delta \mathbf{p})$. In such cases it is possible with little additional cost to compute some sensitivity coefficients u_i together with the solution $S(x,t; \mathbf{p})$. Such an approach would be very advantageous for operators of implicit reservoir simulation codes.

We have examined the accuracy of the approach (8) and (9). A homogeneous reservoir with the following parameter values was investigated: $\phi = 0.25$, $\mu = 4$, $a = b = 2.5$, $S_{wr} = S_{or} = 0.2$, $K_{wm} = K_{om} = 1$, $v = 9.26 \cdot 10^{-7} \text{m/s}$. Let us for example consider perturbations in the parameter $p_3 = b$ and define $u_3 = \partial S / \partial b$. The results showed that u_3 was close to zero in the whole domain, except in a narrow region around the shock in $S(x,t; \mathbf{p})$, where u_3 had a pronounced peak. The height of this peak increased with both N and Δb. The peak extended over two grid points, regardless of the N value (only $N \leq 200$ was tested). The perturbed curve $S^+ = S + u_3 \Delta b$ therefore also displayed a significant overshot around the shock front. With 10% perturbation in b, S^+ represented a qualitative reasonable approximation to $S(x,t; \mathbf{p} + \Delta \mathbf{p})$. Nevertheless, the uncertainties in b are likely to be much larger than 10% and for example 100% increase in b resulted in an S^+ curve which was in poor agreement with $S(x,t; \mathbf{p} + \Delta \mathbf{p})$. Of course we obtained $\lim_{\Delta b \to 0} S^+(x,t; \mathbf{p}) = S(x,t; \mathbf{p} + \Delta \mathbf{p})$. The poor behavior of S^+ is not surprising since a first order Taylor series is employed. The quality of athe approximation then depends on the smoothness of $S(x,t; \mathbf{p})$, and the most inaccurate parts of the S^+ curve is exactly in the shock region of $S(x,t; \mathbf{p})$.

S^+ has also been calculated for perturbations in the other parameters and satisfactory quality of the results was only obtained when the perturbations were uninterestingly small. The use of separate equations for calculating sensitivity coefficients is therefore not generally appropriate in reservoir simulation.

3.3 Results

In this section we present values of perturbations in T due to various perturbations in the input parameters as described in section 3.1. All results are generated by solving the exact differential equations and not by the methods outlined in section 3.2.

Let us first state some preliminary results based on the physics in the problem. Firstly we consider the parameters that enter the Buckley-Leverett problem. Changing the porosity ϕ in a homogeneous medium is equivalent to a linear change in the time scale. Increasing ϕ leads to an increase in T in incompressible flow since the available volume for the fluids becomes larger. Increasing K makes the fluids flow faster and T is then reduced. If we increase a this corresponds to a decrease in water permeability and consequently the time to breakthrough increases. Similarly, if b is increased, the oil permeability is decreased and the time to water breakthrough decreases. Increasing K_{wm} increases the water permeability and has thus the same effect as decreasing a. A similar reasoning yields variations in K_{om}. Graphical discussion of shock velocities in a homogeneous medium based on the fractional flow curve reveals that an increase in S_{wr} or S_{or} leads to a larger shock velocity and hence a decrease in the time to breakthrough is experienced. In the polymer flooding case with monotonic adsorption functions the saturation shock velocity decreases when increasing the slope of A. That is, T increases with increasing ξ and decreases with increasing η. To summarize, we have

$$\frac{\partial T}{\partial \phi} > 0, \quad \frac{\partial T}{\partial a} > 0, \quad \frac{\partial T}{\partial b} < 0, \quad \frac{\partial T}{\partial S_{wr}} < 0, \quad \frac{\partial T}{\partial S_{or}} < 0,$$

$$\frac{\partial T}{\partial K_{wm}} < 0, \quad \frac{\partial T}{\partial K_{om}} > 0, \quad \frac{\partial T}{\partial K} < 0, \quad \frac{\partial T}{\partial \xi} > 0, \quad \frac{\partial T}{\partial \eta} < 0.$$

In all tables we have sorted the parameters after their importance given by the MRI and MRR values. Numerical values are reported with two decimals, and when "0.00" appears, this should be interpreted as a number less than 0.005, but not necessarily zero. All tables in this report are written directly in LaTeX text processing format by the computer in order to minimize typing errors.

Before discussing perturbations in T due to perturbations in input parameters one should clarify the uncertainty in T due to errors in the numerical method. We have performed experiments where $\Delta x \to 0$ and studied the convergence of T. The error in T due to discretization with $N \geq 30$ has never been observed to be larger than 2%. The results in this note are computed with grids where $N = 80$ or $N = 40$. In all calculations we have used $L = 1000$ m, $\kappa = 10^{-11}$ m^2, $\Lambda = 0.01$, $\nu = (\mu_w/\mu_o) = 1/4$, and $\Delta P = 500$ MPa. Unless otherwise stated, polymer is injected during the whole simulation, i.e. $t_s > T$.

3.3.1 Homogeneous reservoir

Consider a homogeneous reservoir, here formally defined by $M = 0$ and p constant in $[0, L]$ with the value p_0. In Table 1 results from pure water flooding, i.e. the standard Buckley–Leverett problem, are presented. The next Tables 2–5 correspond to polymer flooding with different values of ζ (i.e. different mobility ratios). One should observe that increasing Λ, i.e. the polymer concentration, while keeping ζ fixed, will give approximately the same results as increasing ζ, keeping Λ fixed (as is done here). We have used $\zeta = 2$ as a standard value for most simulations in this work. In Table 6 the polymer is injected only for $t_s = 500$ days. The input parameters are perturbed by 50% in Tables 1–6. A perturbation by only 20% gives the results in Table 7. Table 8 corresponds to perturbations larger than 50%, but still physically realistic. Results from polymer injection without adsorption effects are displayed in Table 9. The Tables 6–9 are to be compared with Table 3.

parameter	p_0^{ref}	intervals I_0^j	MRR	MRI
K	1.00	$[0.50, 1.50]$	-0.33	1.00
ϕ	0.20	$[0.10, 0.30]$	-0.50	0.50
a	2.00	$[1.00, 3.00]$	-0.65	0.23
K_{om}	0.60	$[0.30, 0.90]$	-0.20	0.46
K_{wm}	0.60	$[0.30, 0.90]$	-0.17	0.39
S_{or}	0.20	$[0.10, 0.30]$	-0.17	0.17
S_{wr}	0.20	$[0.10, 0.30]$	-0.17	0.17
b	2.00	$[1.00, 3.00]$	-0.02	0.06

AMRR	AMRI	AMRR-F	AMRI-F	AMRR-A	AMRI-A
-0.95	3.80	-0.84	0.59	$-$	$-$

Table 1: Perturbation results for a homogeneous reservoir. $T^{ref} = 788$ days. $\zeta = 0$ (Buckley-Leverett problem).

14

parameter	p_0^{ref}	intervals I_0^j	MRR	MRI
K	1.00	$[0.50, 1.50]$	-0.33	1.00
a	2.00	$[1.00, 3.00]$	-0.72	0.29
ϕ	0.20	$[0.10, 0.30]$	-0.50	0.50
K_{wm}	0.60	$[0.30, 0.90]$	-0.22	0.62
S_{wr}	0.20	$[0.10, 0.30]$	-0.23	0.28
K_{om}	0.60	$[0.30, 0.90]$	-0.12	0.32
S_{or}	0.20	$[0.10, 0.30]$	-0.19	0.20
ξ	0.20	$[0.10, 0.30]$	-0.03	0.04
b	2.00	$[1.00, 3.00]$	0.00	0.05
η	1.00	$[0.50, 1.50]$	-0.02	0.01

AMRR	AMRI	AMRR-F	AMRI-F	AMRR-A	AMRI-A
-0.96	6.98	-0.88	1.54	-0.05	0.04

Table 2: Perturbation results for a homogeneous reservoir. $T^{ref} = 1124$ days. $\zeta = 1$.

parameter	p_0^{ref}	intervals I_0^j	MRR	MRI
K	1.00	$[0.50, 1.50]$	-0.33	1.00
a	2.00	$[1.00, 3.00]$	-0.76	0.31
K_{wm}	0.60	$[0.30, 0.90]$	-0.26	0.78
ϕ	0.20	$[0.10, 0.30]$	-0.50	0.50
S_{wr}	0.20	$[0.10, 0.30]$	-0.25	0.34
S_{or}	0.20	$[0.10, 0.30]$	-0.20	0.21
K_{om}	0.60	$[0.30, 0.90]$	-0.08	0.23
ξ	0.20	$[0.10, 0.30]$	-0.04	0.06
b	2.00	$[1.00, 3.00]$	0.00	0.07
η	1.00	$[0.50, 1.50]$	-0.02	0.01

AMRR	AMRI	AMRR-F	AMRI-F	AMRR-A	AMRI-A
-0.97	8.84	-0.90	2.19	-0.07	0.07

Table 3: Perturbation results for a homogeneous reservoir. $T^{ref} = 1398$ days. $\zeta = 2$.

parameter	p_0^{ref}	intervals I_0^j	MRR	MRI
K_{wm}	0.60	$[0.30, 0.90]$	-0.36	1.25
K	1.00	$[0.50, 1.50]$	-0.33	1.00
a	2.00	$[1.00, 3.00]$	-0.85	0.32
ϕ	0.20	$[0.10, 0.30]$	-0.50	0.50
S_{wr}	0.20	$[0.10, 0.30]$	-0.33	0.53
S_{or}	0.20	$[0.10, 0.30]$	-0.24	0.26
b	2.00	$[1.00, 3.00]$	-0.04	0.19
ξ	0.20	$[0.10, 0.30]$	-0.08	0.12
K_{om}	0.60	$[0.30, 0.90]$	-0.06	0.07
η	1.00	$[0.50, 1.50]$	-0.04	0.03

AMRR	AMRI	AMRR-F	AMRI-F	AMRR-A	AMRI-A
-0.99	9.43	-0.96	3.58	-0.13	0.14

Table 4: Perturbation results for a homogeneous reservoir. $T^{ref} = 3539$ days. $\zeta = 10$.

parameter	p_0^{ref}	intervals I_0^j	MRR	MRI
K_{wm}	0.60	$[0.30, 0.90]$	-0.41	1.20
K	1.00	$[0.50, 1.50]$	-0.33	0.90
a	2.00	$[1.00, 3.00]$	-0.88	0.30
ϕ	0.20	$[0.10, 0.30]$	-0.50	0.49
S_{wr}	0.20	$[0.10, 0.30]$	-0.37	0.60
S_{or}	0.20	$[0.10, 0.30]$	-0.26	0.29
b	2.00	$[1.00, 3.00]$	-0.08	0.23
K_{om}	0.60	$[0.30, 0.90]$	-0.17	0.12
ξ	0.20	$[0.10, 0.30]$	-0.11	0.16
η	1.00	$[0.50, 1.50]$	-0.05	0.03

AMRR	AMRI	AMRR-F	AMRI-F	AMRR-A	AMRI-A
-0.99	6.93	-0.98	2.90	-0.16	0.18

Table 5: Perturbation results for a homogeneous reservoir. $T^{ref} = 7787$ days. $\zeta = 25$.

parameter	p_0^{ref}	intervals I_0^j	MRR	MRI
K	1.00	$[0.50, 1.50]$	-0.29	0.77
a	2.00	$[1.00, 3.00]$	-0.72	0.24
ϕ	0.20	$[0.10, 0.30]$	-0.44	0.39
K_{wm}	0.60	$[0.30, 0.90]$	-0.21	0.51
S_{wr}	0.20	$[0.10, 0.30]$	-0.21	0.25
S_{or}	0.20	$[0.10, 0.30]$	-0.17	0.17
K_{om}	0.60	$[0.30, 0.90]$	-0.08	0.24
ξ	0.20	$[0.10, 0.30]$	-0.03	0.04
b	2.00	$[1.00, 3.00]$	0.02	0.02
η	1.00	$[0.50, 1.50]$	-0.02	0.01

AMRR	AMRI	AMRR-F	AMRI-F	AMRR-A	AMRI-A
-0.96	3.50	-0.89	1.06	-0.05	0.05

Table 6: Perturbation results for a homogeneous reservoir. $T^{ref} = 1228$ days. $\zeta = 2$. Polymer is only injected for a short period, $t_s = 500$ days.

parameter	p_0^{ref}	intervals I_0^j	MRR	MRI
K	1.00	[0.80, 1.20]	−0.17	0.25
ϕ	0.20	[0.16, 0.24]	−0.20	0.20
a	2.00	[1.60, 2.40]	−0.20	0.14
K_{wm}	0.60	[0.48, 0.72]	−0.13	0.19
S_{wr}	0.20	[0.16, 0.24]	−0.11	0.12
S_{or}	0.20	[0.16, 0.24]	−0.08	0.08
K_{om}	0.60	[0.48, 0.72]	−0.04	0.06
ξ	0.20	[0.16, 0.24]	−0.02	0.02
η	1.00	[0.80, 1.20]	−0.01	0.01
b	2.00	[1.60, 2.40]	0.00	0.01

AMRR	AMRI	AMRR-F	AMRI-F	AMRR-A	AMRI-A
−0.62	1.42	−0.42	0.56	−0.03	0.03

Table 7: Perturbation results for a homogeneous reservoir. $T^{ref} = 1398$ days. $\zeta = 2$. In contrast to Tables 1–6, where the input parameters are perturbed by 50%, the perturbation here is only 20%.

parameter	p_0^{ref}	intervals I_0^j	MRR	MRI
K	1.00	[0.10, 10.00]	−0.90	8.78
K_{wm}	0.60	[0.10, 1.00]	−0.31	4.14
a	2.00	[0.50, 6.00]	−0.94	0.80
ϕ	0.20	[0.05, 0.35]	−0.75	0.75
S_{wr}	0.20	[0.00, 0.40]	−0.46	0.87
K_{om}	0.60	[0.10, 1.00]	−0.09	0.93
S_{or}	0.20	[0.00, 0.40]	−0.40	0.44
ξ	0.20	[0.00, 1.00]	−0.19	0.14
b	2.00	[0.50, 6.00]	0.08	0.18
η	1.00	[0.00, 2.00]	−0.05	0.03

AMRR	AMRI	AMRR-F	AMRI-F	AMRR-A	AMRI-A
−	−	−	−	−0.25	0.14

Table 8: Perturbation results for a homogeneous reservoir. $T^{ref} = 1398$ days. $\zeta = 2$. The perturbation of the input parameters are larger than in the Tables 1–7, but still physically reasonable. The AMRR/I values are only given for the adsorption function since the extreme combination of all input parameters in this case is not considered to have practical relevance.

parameter	p_0^{ref}	intervals I_0^j	MRR	MRI
K	1.00	$[0.50, 1.50]$	−0.33	1.00
a	2.00	$[1.00, 3.00]$	−0.78	0.29
K_{wm}	0.60	$[0.30, 0.90]$	−0.26	0.80
ϕ	0.20	$[0.10, 0.30]$	−0.50	0.50
S_{wr}	0.20	$[0.10, 0.30]$	−0.29	0.48
S_{or}	0.20	$[0.10, 0.30]$	−0.21	0.22
K_{om}	0.60	$[0.30, 0.90]$	−0.07	0.21
b	2.00	$[1.00, 3.00]$	0.01	0.07

AMRR	AMRI	AMRR-F	AMRI-F	AMRR-A	AMRI-A
−0.97	7.94	−0.91	2.06	−	−

Table 9: Perturbation results for a homogeneous reservoir. $T^{ref} = 1591$ days. $\zeta = 2$. No adsorption function ($A \equiv 0$).

We may summarize the main results as follows.

- In the Buckley–Leverett problem (Table 1) K, ϕ and a (in this order) are the most important parameters.

- When polymer is injected (Table 2–5), K_{wm} also becomes a significant parameter. Polymer injection has a considerable effect on the ranking of the parameters.

- As ζ increases, the sensitivity in T due to perturbations in a and K_{wm} increases, while the sensitivity due to perturbations in K decreases. The residual saturations, and especially S_{wr}, increase with ζ up to $\zeta = 10$ and thereafter show a slight decrease.

- The influence of the adsorption function parameters ζ and η is fairly small in all our simulations, even in Table 5, where $\zeta = 25$.

- When only a polymer plug is injected (Table 6), the sensitivity in T due to perturbations in K and ϕ is smaller than when polymer is absent (Table 1) or when it is injected during the whole simulation (Table 3).

- The MRR and MRI values of a indicate that the sensitivity of T to perturbations in a is much larger when $a \in [1,2]$ than when $a \in [2,3]$. From Table 8 we see that even larger sensitivities are encountered when $a < 1$. Although we usually have $a > 1$ in two–phase flow, [16] reports laboratory experiments where $a < 1$.

- 50% perturbation in S_{wr}, S_{or}, b, ξ, η, and K_{om} results in a perturbation of T less than 50%. For K_{wm}, a, K, and ϕ the absolute value of either MRR or MRI is likely to exceed 0.5.

- The sensitivity of T due to perturbation of all fractional flow parameter values, represented by AMRR–F and AMRI–F, is significantly larger than the sensitivity of T due to perturbation of porosity or absolute permeability. The importance of F relative to K and ϕ is also considerably larger in polymer flooding compared to pure water flooding. The sensitivity of T to variations in the adsorption function may be considered as negligible. As a conclusion we regard the relative permeability curve of the aqueous phase as the most important source of uncertainties in a polymer flooding problem. Both F and K represent the most important input quantities in pure water flooding.

- Comparison of Tables 3 and 7, as an example, show that 50% perturbation of all parameters in the relative permeability curves gives a variation of T

between 140 and 3075 days, while 20% perturbation leads to $T \in [811, 2181]$ days. The reason why the reduction in T is much larger than than the increase is mainly due the influence of the a and K_{wm} parameters.

3.3.2 Heterogeneous reservoir

The purpose of this section is to give examples of sensitivity measures when the reservoir has space varying rock properties. We assume that the input parameters p are known without uncertainty in the injection and production well, i.e. for $x = 0$ and $x = L$. We have applied two models for the space variation of p between the wells:

- *Discontinuous 3-rock model.* Let $[0, L] = \Omega_0 \cup \Omega_1 \cup \Omega_2$, where

$$\Omega_0 = [0, \frac{1}{4}L], \quad \Omega_1 = [\frac{1}{4}L, \frac{3}{4}L], \quad \Omega_2 = [\frac{3}{4}L, L].$$

The p vector is then assumed to be constant in each Ω_i, $i = 0, 1, 2$, the corresponding values being p_0, p_1 and p_2. All perturbations regard the p_1 values, since p_0 and p_2 correspond to well values without uncertainty.

- *Linear 3-point model.* A coarse "parameter grid", $y_0 = 0$, $y_1 = \frac{1}{2}L$, $y_2 = L$, is introduced. The p vector now vary linearly between the y_i points. Again all perturbations regard the p_1 values.

Figures 2–5 depict the space variations of the input parameters. At first sight it would be natural to let the length of Ω_i in the discontinuous model to $\frac{1}{3}L$. However, with the above chosen values the mean value of p throughout the domain is the same in both the linear and the discontinuous model.

In Tables 10 and 11 the reference values are constant throughout the domain, and the midpoint value p_1 is perturbed by 50%. The two tables correspond to discontinuous and linear space variation of p (cf. Figure 2 and 4). In the next

Figure 2: Discontinuous space variation of a parameter p_i^j. Homogeneous reference values. The thick line indicates the reference value while the thin line represents the perturbed value.
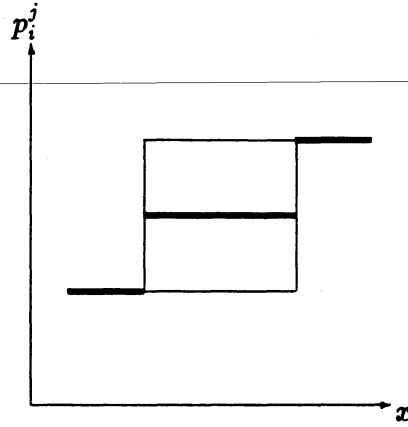
Figure 3: Discontinuous space variation of a parameter p_i^j. Heterogeneous reference values. The thick line indicates the reference value while the thin line represents the perturbed value.

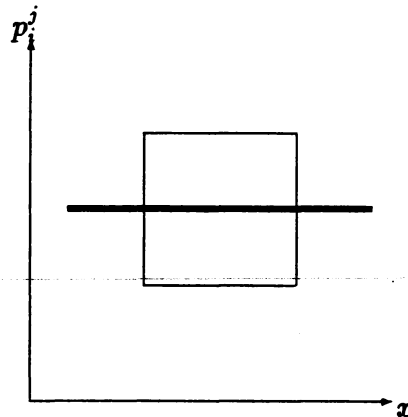
Figure 4: Linear variation of a parameter p_i^j. Homogeneous reference values. The thick line indicates the reference value while the thin line represents the perturbed value.

Figure 5: Linear space variation of a parameter p_i^j. Heterogeneous reference values. The thick line indicates the reference value while the thin line represents the perturbed value.
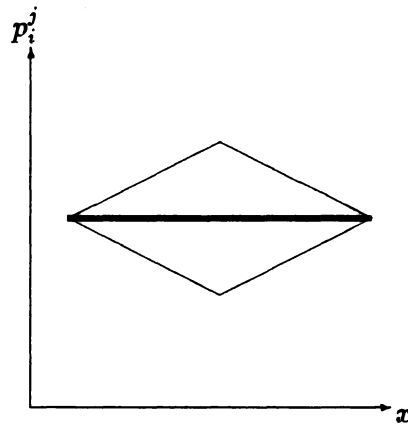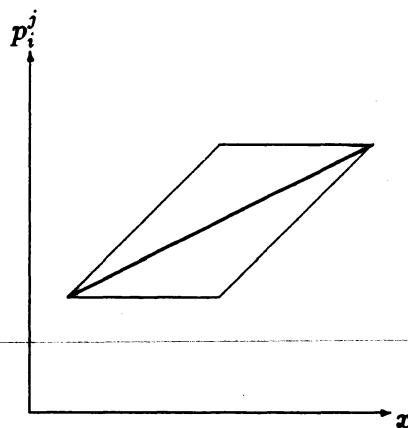
parameter	p_i^{ref}			intervals I_1^j	MRR	MRI
	$i = 0$	$i = 1$	$i = 2$			
ϕ	0.20	0.20	0.20	$[0.10, 0.30]$	-0.20	0.20
K	1.00	1.00	1.00	$[0.50, 1.50]$	-0.09	0.27
a	2.00	2.00	2.00	$[1.00, 3.00]$	-0.22	0.14
K_{wm}	0.60	0.60	0.60	$[0.30, 0.90]$	-0.07	0.17
S_{wr}	0.20	0.20	0.20	$[0.10, 0.30]$	-0.07	0.08
S_{or}	0.20	0.20	0.20	$[0.10, 0.30]$	-0.07	0.07
K_{om}	0.60	0.60	0.60	$[0.30, 0.90]$	-0.02	0.09
b	2.00	2.00	2.00	$[1.00, 3.00]$	-0.01	0.03
ξ	0.20	0.20	0.20	$[0.10, 0.30]$	0.00	0.00
η	1.00	1.00	1.00	$[0.50, 1.50]$	0.00	0.00

AMRR	AMRI	AMRR-F	AMRI-F	AMRR-A	AMRI-A
-0.37	1.89	-0.25	0.60	-0.01	0.00

Table 10: Perturbation results for a heterogeneous reservoir. $T^{ref} = 1398$ days. $\zeta = 2$. Discontinuous space variation of parameters. Homogeneous reference values. The variation of p is depicted in Figure 2.

tables (12–15) the reference values are varying between the two wells. Also here results are presented for both discontinuous and linear variation of p. Tables 12 and 13 show results when the oil is less mobile than the aqueous phase at $x = 0$, while the situation is completely opposite at $x = L$. The contrary problem, with oil as the most mobile phase at $x = 0$, leads to the results displayed in Tables 14 and 15.

The main conclusions from section 3.3.1 are also valid here, and we will now only make a comment on piecewise linear versus piecewise discontinuous space variation of the parameters. In Tables 10 and 11 the reference values of T is of course identical, and the sensitivity measures in these tables can be compared. In particular we notice that perturbations in K have much larger effect on T in the linear model than in the discontinuous one. In Tables 12–15, where the reference parameter values are non–constant, we observe that the type of space variation influences the T^{ref} values and comparison of sensitivity measures from different tables becomes meaningless. However, comparison of T^{ref} values indicates that the type of space variation has a significant impact on the calculations in a deterministic simulator. As the number of points in the coarse parameter grid increases, the influence of the type of space variation of course decreases. In many practical cases where knowledge about the rock properties between the wells is lacking, the present coarse parameter grid is thought to be representative.

Observe that the results obtained here do not apply to general interpolation of quantities in numerical schemes – they are only valid for very coarse meshes, such as those used here for space variation of p.

parameter	$\mathbf{p}_i^{\text{ref}}$			intervals I_1^j	MRR	MRI
	$i=0$	$i=1$	$i=2$			
ϕ	0.20	0.20	0.20	$[0.10, 0.30]$	-0.31	0.31
K	1.00	1.00	1.00	$[0.50, 1.50]$	-0.18	0.42
a	2.00	2.00	2.00	$[1.00, 3.00]$	-0.34	0.21
K_{wm}	0.60	0.60	0.60	$[0.30, 0.90]$	-0.14	0.29
S_{wr}	0.20	0.20	0.20	$[0.10, 0.30]$	-0.14	0.15
S_{or}	0.20	0.20	0.20	$[0.10, 0.30]$	-0.12	0.12
K_{om}	0.60	0.60	0.60	$[0.30, 0.90]$	-0.04	0.13
b	2.00	2.00	2.00	$[1.00, 3.00]$	-0.02	0.04
ξ	0.20	0.20	0.20	$[0.10, 0.30]$	-0.01	0.02
η	1.00	1.00	1.00	$[0.50, 1.50]$	-0.01	0.00

AMRR	AMRI	AMRR-F	AMRI-F	AMRR-A	AMRI-A
-0.67	3.07	-0.48	0.94	-0.02	0.02

Table 11: Perturbation results for a heterogeneous reservoir. $T^{\text{ref}} = 1398$ days. $\zeta = 2$. Linear space variation of parameters. Homogeneous reference values. The variation of p is depicted in Figure 3.

parameter	$\mathbf{p}_i^{\text{ref}}$			intervals I_1^j	MRR	MRI
	$i=0$	$i=1$	$i=2$			
K	0.50	1.00	1.50	$[0.50, 1.50]$	-0.10	0.30
K_{wm}	0.90	0.60	0.30	$[0.30, 0.90]$	-0.08	0.22
ϕ	0.10	0.20	0.30	$[0.10, 0.30]$	-0.12	0.11
S_{wr}	0.10	0.20	0.30	$[0.10, 0.30]$	-0.09	0.09
S_{or}	0.30	0.20	0.10	$[0.10, 0.30]$	-0.06	0.06
a	1.00	2.00	3.00	$[1.00, 3.00]$	-0.06	0.05
K_{om}	0.30	0.60	0.90	$[0.30, 0.90]$	-0.02	0.06
b	3.00	2.00	1.00	$[1.00, 3.00]$	-0.01	0.04
ξ	0.10	0.20	0.30	$[0.10, 0.30]$	-0.02	0.02
η	1.50	1.00	0.50	$[0.50, 1.50]$	-0.01	0.01

AMRR	AMRI	AMRR-F	AMRI-F	AMRR-A	AMRI-A
-0.34	1.19	-0.25	0.33	-0.03	0.02

Table 12: Perturbation results for a heterogeneous reservoir. $T^{\text{ref}} = 2903$ days. $\zeta = 2$. Discontinuous space variation of parameters. Heterogeneous reference values. The variation of p is depicted in Figure 4.

parameter	p_i^{ref}			intervals I_1^j	MRR	MRI
	$i=0$	$i=1$	$i=2$			
K	0.50	1.00	1.50	[0.50, 1.50]	−0.21	0.49
K_{wm}	0.90	0.60	0.30	[0.30, 0.90]	−0.17	0.37
ϕ	0.10	0.20	0.30	[0.10, 0.30]	−0.25	0.25
a	1.00	2.00	3.00	[1.00, 3.00]	−0.27	0.14
S_{wr}	0.10	0.20	0.30	[0.10, 0.30]	−0.16	0.20
S_{or}	0.30	0.20	0.10	[0.10, 0.30]	−0.12	0.12
K_{om}	0.30	0.60	0.90	[0.30, 0.90]	−0.03	0.08
ξ	0.10	0.20	0.30	[0.10, 0.30]	−0.03	0.04
b	3.00	2.00	1.00	[1.00, 3.00]	−0.01	0.03
η	1.50	1.00	0.50	[0.50, 1.50]	−0.01	0.01

AMRR	AMRI	AMRR-F	AMRI-F	AMRR-A	AMRI-A
−0.69	2.65	−0.54	0.76	−0.05	0.05

Table 13: Perturbation results for a heterogeneous reservoir. $T^{ref} = 2236$ days. $\zeta = 2$. Linear space variation of parameters. Heterogeneous reference values. The variation of p is depicted in Figure 5.

parameter	p_i^{ref}			intervals I_1^j	MRR	MRI
	$i=0$	$i=1$	$i=2$			
a	3.00	2.00	1.00	[1.00, 3.00]	−0.25	0.09
ϕ	0.30	0.20	0.10	[0.10, 0.30]	−0.14	0.14
K	1.50	1.00	0.50	[0.50, 1.50]	−0.05	0.15
K_{wm}	0.30	0.60	0.90	[0.30, 0.90]	−0.04	0.07
S_{wr}	0.30	0.20	0.10	[0.10, 0.30]	−0.05	0.05
S_{or}	0.10	0.20	0.30	[0.10, 0.30]	−0.05	0.05
K_{om}	0.90	0.60	0.30	[0.30, 0.90]	−0.01	0.07
b	1.00	2.00	3.00	[1.00, 3.00]	−0.03	0.04
ξ	0.30	0.20	0.10	[0.10, 0.30]	0.00	0.00
η	0.50	1.00	1.50	[0.50, 1.50]	0.00	0.00

AMRR	AMRI	AMRR-F	AMRI-F	AMRR-A	AMRI-A
−0.29	0.97	−0.21	0.37	0.00	0.00

Table 14: Perturbation results for a heterogeneous reservoir. $T^{ref} = 2280$ days. $\zeta = 2$. Discontinuous space variation of parameters. Heterogeneous reference values. The variation of p is depicted in Figure 4.

parameter	p_i^{ref}			intervals I_1^j	MRR	MRI
	$i=0$	$i=1$	$i=2$			
K	1.50	1.00	0.50	$[0.50, 1.50]$	-0.17	0.44
ϕ	0.30	0.20	0.10	$[0.10, 0.30]$	-0.27	0.28
a	3.00	2.00	1.00	$[1.00, 3.00]$	-0.35	0.16
K_{om}	0.90	0.60	0.30	$[0.30, 0.90]$	-0.08	0.26
K_{wm}	0.30	0.60	0.90	$[0.30, 0.90]$	-0.10	0.18
S_{wr}	0.30	0.20	0.10	$[0.10, 0.30]$	-0.11	0.11
S_{or}	0.10	0.20	0.30	$[0.10, 0.30]$	-0.10	0.10
b	1.00	2.00	3.00	$[1.00, 3.00]$	-0.05	0.08
ξ	0.30	0.20	0.10	$[0.10, 0.30]$	-0.01	0.01
η	0.50	1.00	1.50	$[0.50, 1.50]$	0.00	0.00

AMRR	AMRI	AMRR-F	AMRI-F	AMRR-A	AMRI-A
-0.57	2.34	-0.36	0.69	-0.01	0.01

Table 15: Perturbation results for a heterogeneous reservoir. $T^{\mathrm{ref}} = 1656$ days. $\zeta = 2$. Linear space variation of parameters. Heterogeneous reference values. The variation of p is depicted in Figure 5.

4   Stochastic analysis

Since the uncertain input parameters p exhibit a random variation throughout a reservoir it is reasonable to treat these parameters formally as *stochastic random fields*. In practice the governing partial differential equations are solved numerically and they are therefore reduced to sets of linear algebraic equations. Statistically this means that a stochastic random field is discretized to a vector of stochastic variables. The purpose of this part of the note is to apply methods for calculating the statistics of the time T to water breakthrough in the production well. In our case the discretized mathematical model for T consists of sets of algebraic equations where the coefficients are stochastic variables with prescribed distributions.

We will employ recently developed methods from structural reliability for determining the statistics of T and the sensitivity to input parameters. Structural reliability methods have the advantage over sampling techniques (of the Monte-Carlo type) in that sensitivity of probabilities to variations in parameters in both the flow model and the input distributions are cheaply computed. Reliability methods generally give accurate results when the computed probabilities are small. As we will show later, it is likely that reliability methods may be very accurate over the whole range of probabilities in the present reservoir flow problems. Selvig [15] has studied the feasibility of structural reliability methods in reservoir simulation. Selvig used an analytical, one–dimensional, homogeneous, water flooding simulator to demonstrate the principles of the application. Porosity, absolute permeability and irreducible water saturation were chosen as stochastic input variables. In this paper we apply structural reliability methods to the flow problems described in section 3.

We select r of the input parameters p_i^j to be stochastic variables. These variables are denoted by $\mathbf{X} \in \mathbf{R}^r$, $\mathbf{X} = (X_1, \ldots, X_r)^T$, and called *basic variables*. Given statistical information about $\mathbf{X}$ we want to establish statistics of the output T. For this purpose a first order reliability method (FORM) is used. Since this type of analysis is less known to readers of reservoir flow, the next section reviews some of the basic theory. We also introduce notation and definitions and describe how the present problem can be formulated for FORM analysis. The version of FORM used in this note is closely related to that described in [11]. It is referred to Madsen *et al.* [13] for general theory on FORM.

4.1   Theory

Let $\mathbf{X} = (X_1, \ldots, X_r)^T$ be a vector of basic variables. We are interested in computing the probability of the event $\Pr\{g(\mathbf{X}) \leq 0\}$, where $g(\mathbf{X})$ is a *limit state function*. Let $\Omega \in \mathbf{R}^r$ be the set of points where $g \leq 0$ (the *failure domain*).

Clearly the probability can be computed as

$$\Pr\{g(\mathbf{X}) \le 0\} = \int_\Omega f_{\mathbf{X}}(\mathbf{x})dx \qquad (10)$$

where $f_{\mathbf{X}}(\mathbf{x})$ is the joint probability density of the vector $\mathbf{X}$. We will define the limit state function as $g = T - T_\omega$, giving $\Pr\{g \le 0\} = \Pr\{T \le T_\omega\}$, where $T_\omega = \omega\tilde{T}$. $\tilde{T}$ is the deterministic value of T when $E[\mathbf{X}]$ is used as input. Note that T must be computed by solving the differential equations from section 2. There are two problems with the use of (10). Firstly, it may be difficult to establish the joint density, and secondly, the evaluation of the integral, for example by quadrature rules, becomes very expensive, even for moderate values of r. The first problem may be solved to some extent by using methods such as those in [11], which will be discussed below. The second problem can be treated by FORM analysis.

In general it is extremely difficult to assign a joint density to input variables in reservoir simulation. At most we can hope to establish marginal distributions for each basic variable and maybe some correlation coefficients. Let $\Theta_{X_i}(x_i)$ be the marginal distribution function of X_i. The associated density $d\Theta/dx_i$ is denoted by $\theta_{X_i}(x_i)$. If $\mathrm{Cov}[\cdot,\cdot]$ is the covariance operator and $\mathrm{D}[\cdot]$ is the standard deviation operator, the correlation coefficient is

$$\varrho(X_i, X_j) = \frac{\mathrm{Cov}[X_i, X_j]}{\mathrm{D}[X_i]\mathrm{D}[X_j]}.$$

The correlation matrix $\mathbf{R}$ is then $\{\mathbf{R}\}_{ij} = \varrho(X_i, X_j)$. The method used herein restrict the statistical information about the basic variables to only include Θ_{X_i}, $i = 1,\ldots,r$, and $\mathbf{R}$. We refer to [11] for extensions to cases where some or all joint distributions are prescribed.

4.1.1 FORM approximations to probabilities

Let $\langle \mathbf{x}^1, \mathbf{x}^2 \rangle$ be the eucledian inner product of $\mathbf{x}^1, \mathbf{x}^2 \in \mathbf{R}^r$, and let $||\mathbf{x}^1|| = \sqrt{\langle \mathbf{x}^1, \mathbf{x}^1 \rangle}$ be the corresponding norm. In the case where the *failure surface*, defined by $g(\mathbf{X}) = 0$, is a hyperplane, and $f_{\mathbf{X}}(\mathbf{x})$ is a standardized, multivariate normal density,

$$f_{\mathbf{X}}(\mathbf{x}) = \frac{1}{(2\pi)^{r/2}} \exp\left(-\frac{1}{2}||\mathbf{x}||^2\right),$$

the integral in (10) can be calculated analytically:

$$\int_\Omega f_{\mathbf{X}}(\mathbf{x})dx = \Phi(-\beta). \qquad (11)$$

Here Φ is the cumulative, univariate, standardized, normal distribution function, and β is the distance between $\mathbf{X} = 0$ and the (linear) failure surface $g = 0$. Let $\mathbf{x}^*$ be the point on $g = 0$ which is closest to origo ($\mathbf{x}^*$ is called the *design point*). Then $\beta = ||\mathbf{x}^*||$.

To formulate a first order reliability method we consider a mapping

$$\mathbf{X} \to \mathbf{Z} \to \mathbf{Y}$$

such that $\mathbf{Y} = (Y_1, \ldots, Y_r)^T$ is a vector of statistically independent, normally distributed variables with mean zero and unit variance. If the failure surface is linear in the $\mathbf{Y}$-space, the result (11) gives

$$\Pr\{g \le 0\} = \Phi(-\beta), \quad \beta = \|\mathbf{y}^*\| \tag{12}$$

with $\mathbf{y}^*$ as the design point in the $\mathbf{Y}$-space. In the general case where the failure surface is nonlinear (12) holds approximately, i.e. $\Pr\{g \le 0\} \approx \Phi(-\beta)$, provided the curvature of the surface at $\mathbf{y} = \mathbf{y}^*$ is small. The first order reliability method (FORM) refers to this approximate method of calculating $\Pr\{g \le 0\}$.

4.1.2 Transformation of the basic variables

In $\mathbf{Z}$-space the variables are assumed to be jointly normally distributed with correlation matrix $\mathbf{R_0}$, zero mean and unit standard deviation. The mapping $\mathbf{Z} \to \mathbf{Y}$ will therefore be a linear transformation

$$\mathbf{Y} = \mathbf{L_0}^{-1}\mathbf{Z}.$$

$\mathbf{L_0}$ is here the lower triangular Cholesky decomposition of $\mathbf{R_0}$: $\mathbf{R_0} = \mathbf{L_0}\mathbf{L_0}^T$. The mapping $\mathbf{X} \to \mathbf{Z}$ is defined by

$$\Phi(z_i) = \Theta_{X_i}(x_i), \quad i = 1, \ldots, r. \tag{13}$$

In addition the $\mathbf{R}$ matrix must be transformed to $\mathbf{R_0}$. This may be done approximately by empirically based formulas (see [11]) for a wide range of distributions Θ_{X_i}. However, we will exclusively be concerned with normally or lognormally distributed variables in $\mathbf{X}$-space. In this case the transformation (13) and the formulas for transforming $\mathbf{R}$ to $\mathbf{R_0}$ can be simplified and made exact. Let $\{\mathbf{R_0}\}_{ij} = \varrho(Z_i, Z_j)$. If X_i is normally distributed with mean $\mathrm{E}[X_i]$ and standard deviation $\mathrm{D}[X_i]$, we have

$$Z_i = \frac{X_i - \mathrm{E}[X_i]}{\mathrm{D}[X_i]}.$$

If both X_i and X_j are normal variables, $\varrho(Z_i, Z_j) = \varrho(X_i, X_j)$. For a lognormally distributed variable X_i the transformation (13) simplifies to

$$Z_i = \frac{\ln X_i - \mathrm{E}[\ln X_i]}{\mathrm{D}[\ln X_i]},$$

and $\varrho(Z_i, Z_j) = \lambda\varrho(X_i, X_j)$, where

$$\lambda = \frac{\ln(1 + \varrho(X_i, X_j)\delta_i\delta_j)}{\varrho(X_i, X_j)\sqrt{\ln(1 + \delta_i^2)\ln(1 + \delta_j^2)}} \tag{14}$$

when both X_i and X_j are lognormally distributed. The coefficient of variation, δ_i, is defined as

$$\delta_i = \frac{D[X_i]}{E[X_i]}.$$

If X_i is normally distributed and X_j is lognormally distributed, we have

$$\lambda = \frac{\delta_j}{\sqrt{\ln(1 + \delta_j^2)}}. \tag{15}$$

The formulas (14) and (15) are exact. It is remarked that the joint normal distribution of $\mathbf{Z}$ is of course an assumption and implies a certain joint density of $\mathbf{X}$. This joint density is in general different from the exact joint density which is unknown, but the two densities have the same correlation matrix $\mathbf{R}$. The basic assumption is that the distribution is characterized to a large extent by second-order statistics. Notice that uncorrelated basic variables imply stochastically independent variables when we use the transformation $\mathbf{X} \rightarrow \mathbf{Z}$ described above.

4.1.3 Determination of the design point

Let $g_y(\mathbf{y})$ be the limit state function in $\mathbf{Y}$–space. The design point $\mathbf{y}^*$ is the solution of the constrained minimization problem

$$\mathbf{y}^* = \min_{g_y = 0} \|\mathbf{y}\|.$$

There will generally be several local minima of the distance to the failure surface. The computation of a local minimum is carried out by a standard procedure ([11], [13]). In this work we iterate in $\mathbf{X}$-space and linearize the transformation $\mathbf{X} \rightarrow \mathbf{Y}$ in each iteration. Define the vector $\widehat{\mathbf{M}} = (\hat{\mu}_1, \ldots, \hat{\mu}_r)^T$ and the matrix $\widehat{\mathbf{D}} = \mathrm{diag}(\hat{\sigma}_i, \ldots, \hat{\sigma}_r)$. Given an initial guess $\mathbf{x}^0 = (x_1^0, \ldots, x_r^0)^T$ for the design point in $\mathbf{X}$-space we iterate for $\ell = 0, 1, \ldots$ as follows:

$$\hat{\sigma}_i^\ell = \frac{\varphi\left\{\Phi^{-1}\left[\Theta_{X_i}(x_i^\ell)\right]\right\}}{\theta_{X_i}(x_i^\ell)}, \quad i = 1, \ldots, r \tag{16}$$

$$\hat{\mu}_i^\ell = x_i^\ell - \hat{\sigma}_i^\ell \Phi^{-1}\left[\Theta_{X_i}(x_i^\ell)\right], \quad i = 1, \ldots, r \tag{17}$$

$$\mathbf{Q}^\ell = \widehat{\mathbf{D}}^\ell \mathbf{R}_0 \widehat{\mathbf{D}}^\ell \tag{18}$$

$$\mathbf{x}^{\ell+1} = \widehat{\mathbf{M}}^\ell + \frac{\left\langle \mathbf{x}^\ell - \widehat{\mathbf{M}}^\ell, \nabla_x g(\mathbf{x}^\ell)\right\rangle - g(\mathbf{x}^\ell)}{\left\langle \nabla_x g(\mathbf{x}^\ell), \mathbf{Q}^\ell \nabla_x g(\mathbf{x}^\ell)\right\rangle} \mathbf{Q}^\ell \nabla_x g(\mathbf{x}^\ell) \tag{19}$$

$$\mathbf{y}^{\ell+1} = \mathbf{L}_0^{-1}\left[\widehat{\mathbf{D}}^\ell\right]^{-1}\left(\mathbf{x}^{\ell+1} - \widehat{\mathbf{M}}^\ell\right) \tag{20}$$

$$\beta^{\ell+1} = \sqrt{\left\langle \mathbf{y}^{\ell+1}, \mathbf{y}^{\ell+1}\right\rangle} \tag{21}$$

In these equations ∇_x is the gradient operator in $\mathbf{X}$–space, that is,

$$\nabla_x = \left(\frac{\partial}{\partial x_1}, \ldots, \frac{\partial}{\partial x_r}\right)^T.$$

φ denotes the univariate normal density function with zero mean and unit variance. Equation (20) shows that $\widehat{\mathbf{M}}$ and $\widehat{\mathbf{D}}$ can be interpreted as instantaneous/equivalent mean and standard deviation of $\mathbf{X}$. In fact, when $\mathbf{X}$ are jointly normally distributed, $\widehat{\mathbf{M}}$ and $\widehat{\mathbf{D}}$ contain the means and standard deviations, respectively. Since the value of g is a result of a numerical solution of partial differential equations, the gradient $\nabla_x g$ of g with respect to the basic variables must be computed numerically. In each iteration the algorithm above therefore requires $r+1$ evaluations of $g = T - T_\omega$. The iteration is stopped when $|\beta^{\ell+1} - \beta^\ell| \leq \epsilon_\beta$, where for our purposes $\epsilon_\beta = 0.01$ suffices. Having found β, we utilize the approximation

$$\Pr\{g(\mathbf{X}) \leq 0\} \approx \begin{cases} \Phi(-\beta) & g(\mathbf{x}^*) > 0, \\ \Phi(\beta) & g(\mathbf{x}^*) \leq 0. \end{cases}$$

One may notice that if $\mathbf{X}$ is jointly normally distributed β coincides with the Hasofer–Lind reliability index [13].

4.1.4   Sensitivity measures

One of the attractive features of FORM is that one can compute sensitivity coefficients very efficiently. Let the transformation $\mathbf{X} \to \mathbf{Y}$ be denoted by $\mathbf{Y} = \mathbf{T}(\mathbf{X}; \mathrm{E}[\mathbf{X}], \mathrm{D}[\mathbf{X}])$. Then we have

$$\frac{\partial \beta}{\partial \mathrm{E}[\mathbf{X}]} = \frac{1}{\beta} \left\langle \mathbf{y}^*, \frac{\partial}{\partial \mathrm{E}[\mathbf{X}]} \mathbf{T}(\mathbf{x}^*; \mathrm{E}[\mathbf{X}], \mathrm{D}[\mathbf{X}]) \right\rangle \tag{22}$$

and

$$\frac{\partial \beta}{\partial \mathrm{D}[\mathbf{X}]} = \frac{1}{\beta} \left\langle \mathbf{y}^*, \frac{\partial}{\partial \mathrm{D}[\mathbf{X}]} \mathbf{T}(\mathbf{x}^*; \mathrm{E}[\mathbf{X}], \mathrm{D}[\mathbf{X}]) \right\rangle \tag{23}$$

The limit state function may contain a set of parameters $\mathbf{r}$ besides the basic variables $\mathbf{X}$: $g = g(\mathbf{X}; \mathbf{r})$. In our case $\mathbf{r}$ may be input variables which are not treated stochastically. It can be shown that

$$\frac{\partial \beta}{\partial \mathbf{r}} = \frac{\frac{\partial}{\partial \mathbf{r}} g(\mathbf{x}^*; \mathbf{r})}{\sqrt{\langle \nabla_x g(\mathbf{x}^*), \mathbf{Q}^* \nabla_x g(\mathbf{x}^*) \rangle}} \tag{24}$$

$\mathbf{Q}^*$ is the value of $\mathbf{Q}$ in the last iteration. Strictly speaking, the sensitivity coefficients above are approximately correct and approach the exact coefficients as $\beta \to \infty$. It is important to remark that the gradients of g with respect to limit state function parameters or distribution parameters must be determined numerically in our application. In practice we are often interested in the sensitivity of $\Pr\{T \leq T_\omega\}$ to distribution or limit state function parameters. Such quantities are obtained straightforwardly:

$$\Upsilon_E \equiv \frac{\partial}{\partial \mathrm{E}[\mathbf{X}]} \Pr\{T \leq T_\omega\} = \varphi(\beta) \frac{\partial \beta}{\partial \mathrm{E}[\mathbf{X}]},$$

$$\Upsilon_D \equiv \frac{\partial}{\partial D[\mathbf{X}]} \Pr\{T \le T_\omega\} = \varphi(\beta)\frac{\partial\beta}{\partial D[\mathbf{X}]},$$

$$\Upsilon_R \equiv \frac{\partial}{\partial \mathbf{r}} \Pr\{T \le T_\omega\} = \varphi(\beta)\frac{\partial\beta}{\partial \mathbf{r}}.$$

Define the unit vector $\alpha = (\alpha_1, \ldots, \alpha_r)^T$ as $\alpha = \mathbf{y}^*/\beta$, The quantities $\alpha_1^2, \ldots, \alpha_r^2$ are termed *importance factors* and since $\sum_{i=1}^r \alpha_i^2 = 1$, α_i^2 reflects the relative importance of $\mathbf{X}_i$ in determination of β or $\Pr\{g \le 0\}$.

Omission sensitivity factors reflect the error in β when one of the basic variables $\mathbf{X}_i$ is treated as a constant with value equal to, say the median $\bar{m}_i$ of $\mathbf{X}_i$. Generally we have

$$\gamma_i \equiv \frac{1}{\sqrt{1 - \alpha_i^2}} \rightarrow \frac{\beta(\mathbf{X}_i = \bar{m}_i)}{\beta}, \quad \alpha_i^2 \rightarrow 0. \tag{25}$$

Thus, when γ_i is close to unity, the variable X_i contributes very little to β (or $\Pr\{g \le 0\}$) and may be omitted from the stochastic analysis and instead replaced by its median value. By checking the γ_i values in the first iteration one can omit several stochastic variables and thereby increase the efficiency of the analysis considerably. Recall that $r + 1$ solutions of the partial differential equations are required in each iteration. In many cases, as will be shown later, only a few basic variables contribute significantly to the determination of β.

4.2 Examples of failure surfaces in reservoir flow

Recall that accuracy of FORM depends on the curvature of the failure surface $g = 0$ at the design point in Y-space. If the failure surface is approximately linear, $\Phi(-\beta)$ will be a very good approximation to $\Pr\{g \leq 0\}$. There may frequently be many local minima of the distance to the failure surface, and the computation of the probabilities is then more complicated and expensive ([13]).

To gain insight into the quality of the FORM approximations in the present problem we have plotted contour lines of the limit state function when there are two basic variables. As physical problem the homogeneous flow case in section 3.3.1 was chosen. Parameter values were as in Table 3. The expectation of a basic variable equals here the reference value in Table 3, and the coefficient of variation is chosen as $1/3$. $T_\omega = T_{0.8} = 1123$ days. Figure 6 shows g as a function of a and b in X-space and as a function of transformed variables in Y-space. A lognormal distribution is assigned to a and b. The variables are uncorrelated. At this point it would be natural to introduce additional symbols to distinguish deterministic and stochastic quantities. However, with the widely used notation which is employed here for the input parameters no simple rule (e.g. upper case stochastic variables, lower case deterministic variables) seems applicable. It should nevertheless be clear from the context whether a variable is stochastic or deterministic. In Figure 7 we have plotted g as a function of S_{wr} and S_{or}. These basic variables are lognormally distributed with correlation coefficient $\varrho(S_{wr}, S_{or}) = 0.5$. Figure 8 visualizes g as a function of K_{wm} and K_{om}. These two basic variables are uncorrelated and lognormally distributed. Finally in Figure 9, g is plotted as a function of ϕ and K, where $\varrho(\phi, K) = 0.8$, and ϕ is normally distributed while K has a lognormal distribution function.

The plots of $g(X)$ give an indication of how T varies with a, b, S_{wr}, S_{or}, K_{wm}, K_{om}, ϕ and K, that can be of interest with respect to interpretation of the results from a deterministic simulator.

From the plot of g in Y-space we see that the failure surfaces, which correspond to the contour lines of g, are approximately linear. This indicates high accuracy of FORM probabilities. We also see that there are not more than one local minimum of the distance to the failure surface, and the formulas presented previously are sufficient for calculating probabilities.

Figure 6: The limit state function $g = T - T_\omega$ as a function of $X_1 = a$ and $X_2 = b$ (left) and the corresponding transformed variables Y_1 and Y_2 (right). $\varrho(a, b) = 0$.

Figure 7: The limit state function $g = T - T_\omega$ as a function of $X_1 = S_{wr}$ and $X_2 = S_{or}$ (left) and the corresponding transformed variables Y_1 and Y_2 (right). $\varrho(S_{wr}, S_{or}) = 0$.

Figure 8: The limit state function $g = T - T_\omega$ as a function of $X_1 = K_{wm}$ and $X_2 = K_{om}$ (left) and the corresponding transformed variables Y_1 and Y_2 (right). $\varrho(K_{wm}, K_{om}) = 0$.
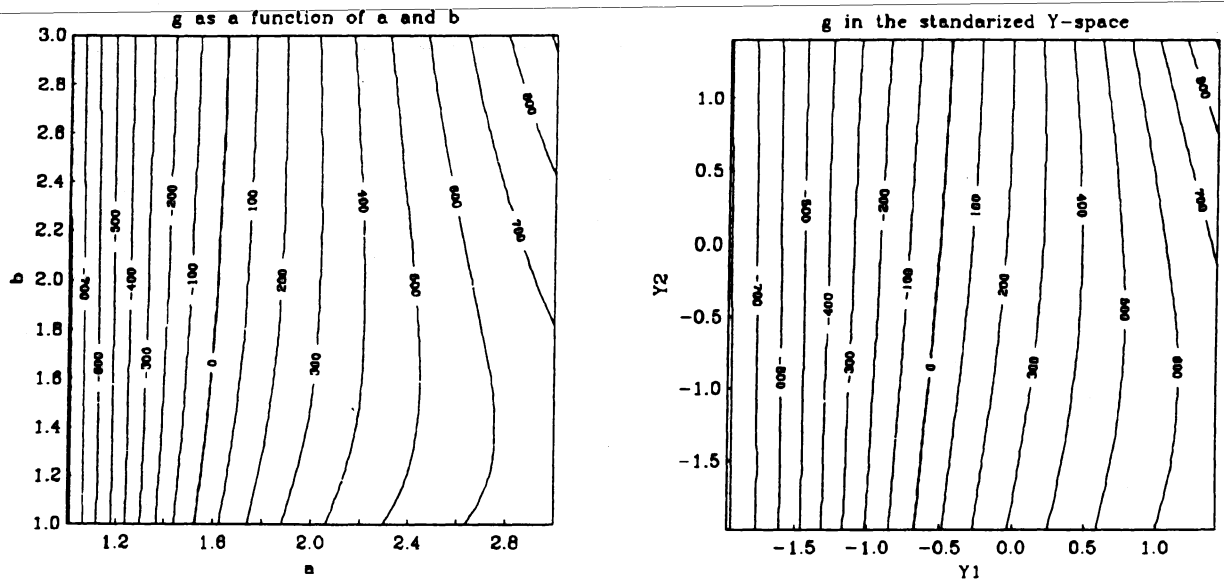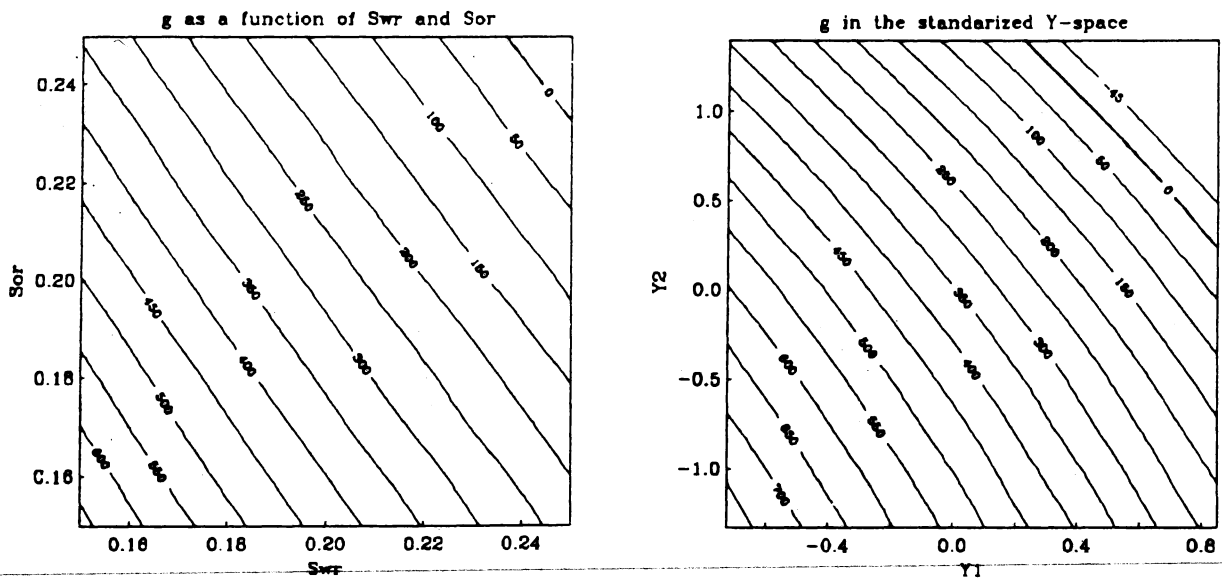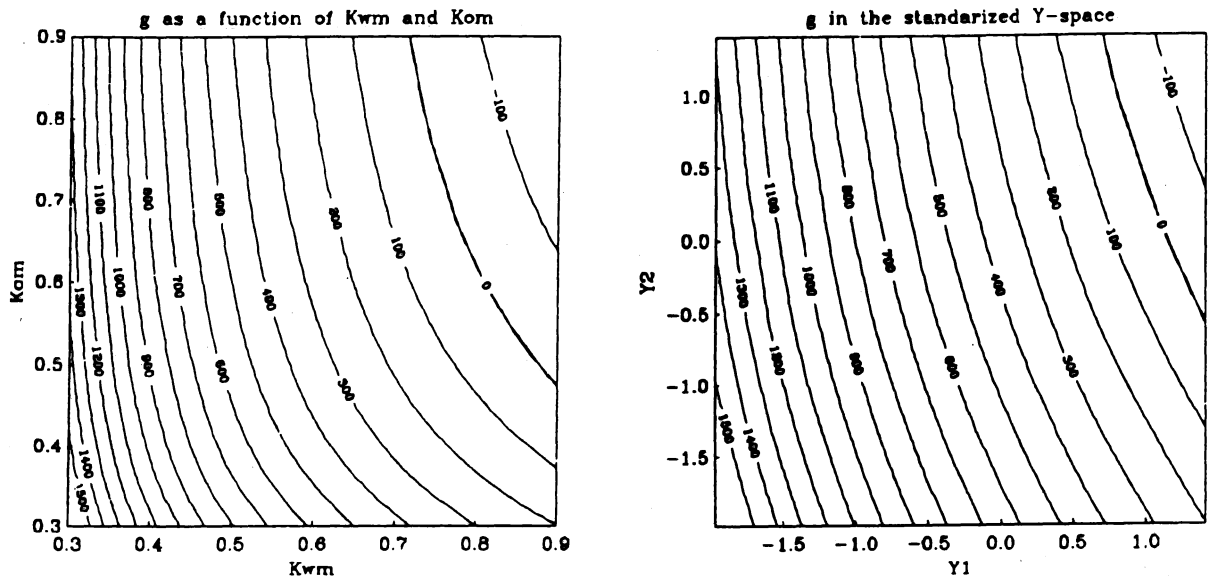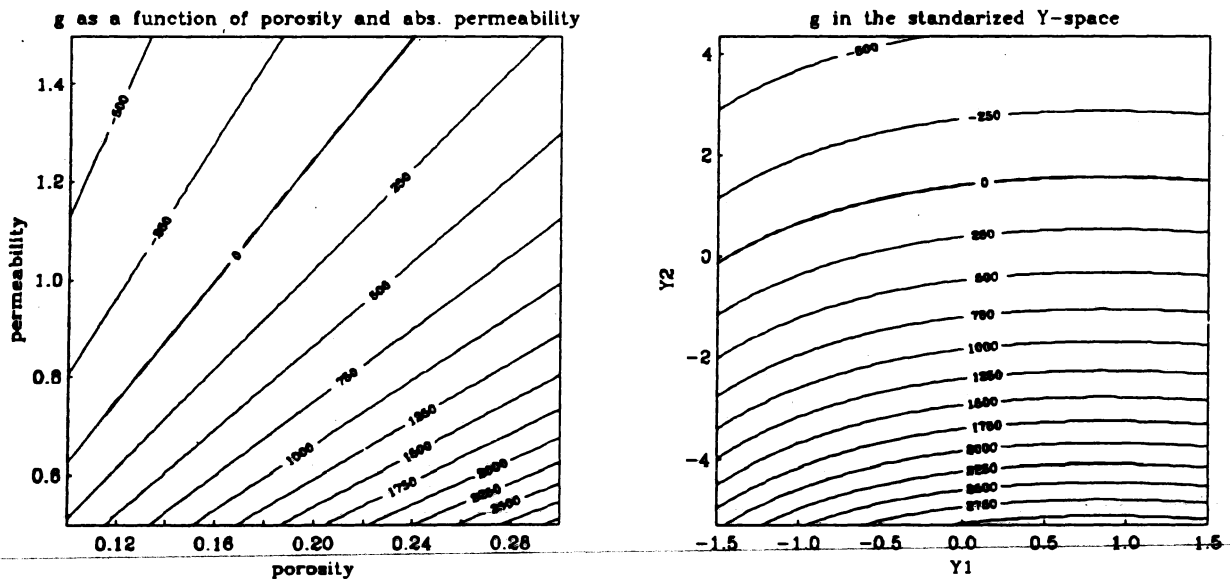

Figure 9: The limit state function $g = T - T_\omega$ as a function of $X_1 = \phi$ and $X_2 = K$ (left) and the corresponding transformed variables Y_1 and Y_2 (right). $\varrho(\phi, K) = 0.8$.

4.3 Results

We start with reporting some information on the numerical performance of the search algorithm. It is important to note that T is not a smooth function of the input parameters when the partial differential equations are discretized: T can only be determined as $m\Delta t$, m being an integer. This property influences the computation of derivatives of the limit state function $g = T - T_\omega$. For example, consider the calculation of $\partial g/\partial x_1$ by

$$\frac{\partial g}{\partial x_1} \approx \frac{1}{\epsilon}[g(x_1 + \epsilon, x_2, \ldots, x_r) - g(x_1, \ldots, x_r)].$$

If ϵ is so small that $g(x_1 + \epsilon, x_2, \ldots, x_r) - g(x_1, \ldots, x_r) \leq \Delta t$, we will obtain $\partial g/\partial x_1 = 0$ when g is found from a numerical scheme for the partial differential equations. Even if ϵ is large enough to prevent vanishing derivative, convergence problems of the search algorithm may occur. Of course, the value of ϵ when computing $\partial g/\partial x_i$ depends on the magnitude of x_i. We have scaled all basic variables such that their magnitudes are of order unity. In this work we have obtained good results with $\epsilon = 0.1$ for all basic variables. In general the convergence rate of the search algorithm depends on ω. When $\omega \in [1/2, 2]$ the convergence is fast, usually 3–4 iterations. Convergence problems may occur when ω is outside this interval.

A natural way of organizing the stochastic analysis in accordance with the deterministic one would be to choose E[**X**] as the reference values in the deterministic case, assign the same coefficient of variation to all X_i, and then finally report the coefficient of variation of T. Such an approach requires construction of the probability density of T. Since one FORM computation produces one point on the cumulative T distribution curve, one needs at least 10 such points to determine the standard deviation and expectation of T. With 4 iterations per FORM calculation and 8 basic variables, each physical problem then requires 360 solutions of the partial differential equations. For reference we suggest the following procedure for calculating moments of T. Let $\Theta_T(t)$, $t_0 \leq t \leq t_n$, be the marginal distribution of T, and assume that $\Theta_i \equiv \Theta_T(t_i)$, is known for some t_i, $i = 0, \ldots, n$. Then integration by parts in the definition of the moments gives

$$\mathrm{E}[T^s] = t_n^s - \int_{t_0}^{t_n} s t^{s-1}\Theta_T(t)dt.$$

Employing Simpson's rule for integration we may write

$$\mathrm{E}[T^s] = t_n^s - \frac{1}{6}\left(t_n - t_{n-2} + \sum_{i=2,4,6,\ldots}(t_{i+2} - t_{i-2})s t_i^{s-1}\Theta_i + 4\sum_{i=1,3,5,\ldots}(t_{i+1} - t_{i-1})s t_i^{s-1}\Theta_i\right).$$

To avoid very large computational cost we have only computed the probability that the time to breakthrough is 20% less than the deterministic reference values provided in section 3 (i.e. $\omega = 0.8$). This is the information about the uncertainty

in T which will be presented. A practical interpretation of the reported probabilities is that they (approximately) represent the risk of under predicting the oil production until water breakthrough by more than 20%.

4.3.1 Homogeneous reservoir

We consider the same physical problem as in section 3.3.1, i.e. a homogeneous reservoir. The basic variables are defined as

$$X_1 = \phi, \quad X_2 = a, \quad X_3 = b, \quad X_4 = S_{wr},$$

$$X_5 = S_{or}, \quad X_6 = K_{wm}, \quad X_7 = K_{om}, \quad X_8 = K.$$

Since the influence of uncertainties in ξ and η is fairly small, we treat these parameters deterministicly. In accordance with common practice the porosity is assumed to be normally distributed whereas the absolute permeability is assigned a lognormal distribution. The other basic variables can attain positive values only. Due to lack of better knowledge we let these be lognormally distributed. The expectation $E[\mathbf{X}]$ is chosen equal to the reference values in section 3.3.1, and the standard variation follows from assigning a coefficient of variation δ_i to each basic variable.

Table 16 displays the results for uncorrelated basic variables while Table 17 gives the results for the case when the basic variables are correlated. The sign of correlation coefficients are chosen in accordance with the physics of the problem. It is remarked that the entries in $\mathbf{R}$ must be chosen so that $\mathbf{R}_0$ becomes positive definite, for example, correlation coefficients $\varrho(X_i, X_j)$ close to ± 1 must be avoided, as these may result in $|\varrho(Z_i, Z_j)| > 1$. If a high correlation (e.g. $\varrho(X_i, X_j) \geq 0.7$) is assigned for many of the basic variables convergence problems of the algorithm (16)–(21) may occur. In the tables the k in the second column refers to the coarse grid point where the basic variable is defined. The present problem is homogeneous and the k value is irrelevant. We have run the problem in Tables 16 and 17 for several values of ω, and Figure 10 shows the probability distribution of T in the correlated and the uncorrelated case. Table 18 displays results from the Buckley-Leverett problem. If $\mathbf{X}$ is jointly normally distributed, we obtain the results listed in Table 19. Table 20 shows results where all basic variables for which $\gamma_i \leq 1.03$ after the first iteration are omitted from the stochastic analysis. This table should be compared to Table 17. In Tables 16–20 the coefficient of variation δ_i equals 1/3. Tables 21 presents results when $\delta_i = 0.1$. Tables 23 and 22 show results for uncorrelated and correlated variables, respectively, when $\delta_i = 0.1$ for all variables, except for K where $\delta_i = 1/2$. This choice of the coefficient of variation is intended to model the fact that uncertainties in K is usually larger than uncertainties in the other basic variables.

parameter	k	E[X]	D[X]	x*	α_i^2	γ_i	Υ_E	Υ_D	omitted?
ϕ	0	0.20	0.067	0.18	0.39	1.28	3.29	−0.18	no
a	0	2.00	0.667	1.77	0.19	1.11	0.29	−0.09	no
b	0	2.00	0.667	1.90	0.00	1.00	−0.01	0.00	no
S_{wr}	0	0.20	0.067	0.20	0.08	1.04	−2.31	0.15	no
S_{or}	0	0.20	0.067	0.20	0.05	1.02	−1.82	0.12	no
K_{wm}	0	0.60	0.200	0.60	0.12	1.06	−0.76	0.08	no
K_{om}	0	0.60	0.200	0.58	0.00	1.00	−0.16	0.02	no
K	0	1.00	0.333	1.02	0.17	1.10	−0.52	0.05	no

Table 16: Physical problem as in Table 3. E[X] equals p_i^{ref} in Table 3, and $\delta_i = 1/3$ for all variables. No correlation between the basic variables. $\beta = 0.51$, $\Pr\{T \le T_{0.80}\} = \Pr\{T \le 1119\} = 0.30$, 3 iterations.

parameter	k	E[X]	D[X]	x*	α_i^2	γ_i	Υ_E	Υ_D	omitted?
ϕ	0	0.20	0.067	0.18	0.22	1.13	2.46	−0.10	no
a	0	2.00	0.667	1.69	0.42	1.31	0.44	−0.16	no
b	0	2.00	0.667	1.83	0.04	1.02	0.13	−0.03	no
S_{wr}	0	0.20	0.067	0.22	0.13	1.07	−2.84	0.12	no
S_{or}	0	0.20	0.067	0.21	0.11	1.06	−2.64	0.11	no
K_{wm}	0	0.60	0.200	0.59	0.08	1.04	−0.62	0.07	no
K_{om}	0	0.60	0.200	0.57	0.00	1.00	−0.03	0.00	no
K	0	1.00	0.333	0.94	0.01	1.01	−0.14	0.03	no

Table 17: Physical problem as in Table 3. E[X] equals p_i^{ref} in Table 3, and $\delta_i = 1/3$ for all variables. $\varrho(\phi, a) = 0.1$, $\varrho(\phi, b) = 0.1$, $\varrho(\phi, S_{wr}) = -0.4$, $\varrho(\phi, S_{or}) = -0.4$, $\varrho(\phi, K_{wm}) = 0.1$, $\varrho(\phi, K_{om}) = 0.1$, $\varrho(\phi, K) = 0.8$. $\beta = 0.51$, $\Pr\{T \le T_{0.80}\} = \Pr\{T \le 1119\} = 0.31$, 3 iterations.
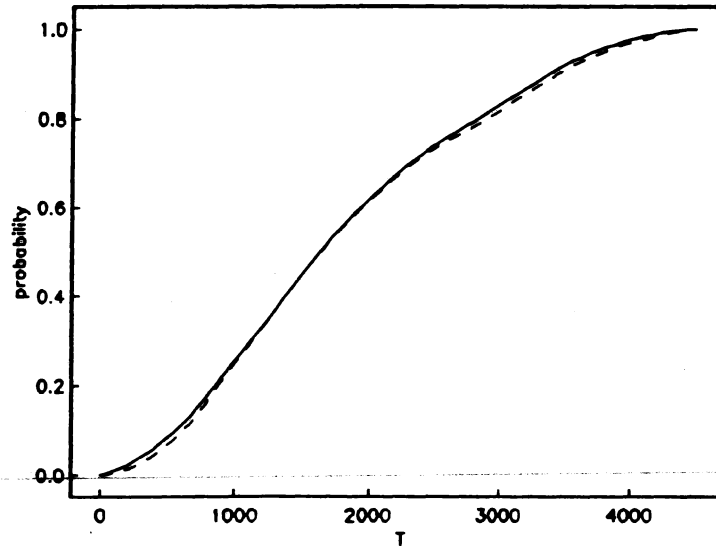

Figure 10: Probability distribution $\Theta_T(t) = \Pr\{T \le t\}$ for the time T to water breakthrough. The physical problem corresponds to that in Tables 16 and 17. The solid line represents correlated variables while the dashed line represents uncorrelated variables.

parameter	k	E[X]	D[X]	x^*	α_i^2	γ_i	Υ_E	Υ_D	omitted?
ϕ	0	0.20	0.067	0.18	0.25	1.15	2.47	−0.13	no
a	0	2.00	0.667	1.66	0.38	1.27	0.41	−0.16	no
b	0	2.00	0.667	1.82	0.03	1.01	0.10	−0.03	no
S_{wr}	0	0.20	0.067	0.22	0.12	1.07	−2.53	0.09	no
S_{or}	0	0.20	0.067	0.22	0.14	1.08	−2.71	0.09	no
K_{wm}	0	0.60	0.200	0.59	0.04	1.02	−0.44	0.05	no
K_{om}	0	0.60	0.200	0.59	0.03	1.01	−0.36	0.04	no
K	0	1.00	0.333	0.93	0.02	1.01	−0.16	0.03	no

Table 18: Buckley-Leverett problem (pure water flooding). E[X] equals p_i^{ref} in Table 1, and $\delta_i = 1/3$ for all variables. Correlations as in Table 17. $\beta = 0.61$, $\Pr\{T \le T_{0.80}\} = \Pr\{T \le 617\} = 0.27$, 3 iterations.

parameter	k	E[X]	D[X]	x^*	α_i^2	γ_i	Υ_E	Υ_D	omitted?
ϕ	0	0.20	0.067	0.19	0.20	1.12	2.53	−0.07	no
a	0	2.00	0.667	1.85	0.42	1.32	0.37	−0.06	no
b	0	2.00	0.667	1.95	0.04	1.02	0.12	−0.01	no
S_{wr}	0	0.20	0.067	0.22	0.14	1.08	−2.08	−0.09	no
S_{or}	0	0.20	0.067	0.22	0.12	1.06	−1.93	−0.08	no
K_{wm}	0	0.60	0.200	0.62	0.07	1.04	−0.50	−0.02	no
K_{om}	0	0.60	0.200	0.60	0.00	1.00	−0.07	0.00	no
K	0	1.00	0.333	1.00	0.01	1.01	−0.13	0.00	no

Table 19: In contrast to Table 17 all variables are here normally distributed. Correlations as in Table 17. $\beta = 0.33$, $\Pr\{T \le T_{0.80}\} = \Pr\{T \le 1119\} = 0.37$, 2 iterations.

parameter	k	E[X]	D[X]	x^*	α_i^2	γ_i	Υ_E	Υ_D	omitted?
ϕ	0	0.20	0.067	0.18	0.40	1.29	3.29	-0.19	no
a	0	2.00	0.667	1.76	0.20	1.11	0.29	-0.09	no
b	0	2.00	0.667	1.89	0.00	1.00	0.00	0.00	yes
S_{wr}	0	0.20	0.067	0.20	0.08	1.04	-2.31	0.15	no
S_{or}	0	0.20	0.067	0.20	0.05	1.02	-1.80	0.12	no
K_{wm}	0	0.60	0.200	0.60	0.11	1.06	-0.75	0.08	no
K_{om}	0	0.60	0.200	0.56	0.00	1.00	0.12	-0.02	yes
K	0	1.00	0.333	1.02	0.17	1.10	-0.51	0.05	no

Table 20: Physical problem as in Table 3. E[X] equals p_i^{ref} in Table 3, and $\delta_i = 1/3$ for all variables. Basic variables for which $\gamma_i \leq 1.03$ after the first iteration, are omitted from the stochastic analysis. Uncorrelated basic variables. $\beta = 0.51$, $\Pr\{T \leq T_{0.80}\} = \Pr\{T \leq 1119\} = 0.30$, 4 iterations.

parameter	k	E[X]	D[X]	x^*	α_i^2	γ_i	Υ_E	Υ_D	omitted?
ϕ	0	0.20	0.020	0.19	0.21	1.12	4.58	-0.15	no
a	0	2.00	0.200	1.84	0.39	1.28	0.73	-0.23	no
b	0	2.00	0.200	1.93	0.05	1.03	0.25	-0.04	no
S_{wr}	0	0.20	0.020	0.22	0.14	1.08	-5.56	-0.06	no
S_{or}	0	0.20	0.020	0.22	0.12	1.07	-5.16	-0.05	no
K_{wm}	0	0.60	0.060	0.62	0.07	1.04	-1.09	0.00	no
K_{om}	0	0.60	0.060	0.60	0.00	1.00	-0.14	0.01	no
K	0	1.00	0.100	0.99	0.01	1.01	-0.25	0.02	no

Table 21: Physical problem as in Table 3. E[X] equals p_i^{ref} in Table 3, and $\delta_i = 0.1$ for all variables. Correlations as in Table 17. $\beta = 1.17$, $\Pr\{T \leq T_{0.80}\} = \Pr\{T \leq 1119\} = 0.12$, 4 iterations.

parameter	k	E[X]	D[X]	x^*	α_i^2	γ_i	Υ_E	Υ_D	omitted?
ϕ	0	0.20	0.020	0.20	0.07	1.04	4.13	-0.04	no
a	0	2.00	0.200	1.97	0.03	1.02	0.30	-0.03	no
b	0	2.00	0.200	1.99	0.00	1.00	0.00	0.00	no
S_{wr}	0	0.20	0.020	0.20	0.02	1.01	-3.33	0.07	no
S_{or}	0	0.20	0.020	0.20	0.01	1.01	-2.60	0.05	no
K_{wm}	0	0.60	0.060	0.60	0.02	1.01	-0.97	0.03	no
K_{om}	0	0.60	0.060	0.60	0.00	1.00	-0.28	0.01	no
K	0	1.00	0.500	1.20	0.85	2.56	-0.63	-0.01	no

Table 22: Physical problem as in Table 3. E[X] equals p_i^{ref} in Table 3, and $\delta_i = 0.1$ for all variables, except for K which has a coefficient of variation equal to 1/2. Uncorrelated variables. $\beta = 0.68$, $\Pr\{T \leq T_{0.80}\} = \Pr\{T \leq 1119\} = 0.25$, 4 iterations.

parameter	k	E[**X**]	D[**X**]	x^*	α_i^2	γ_i	Υ_E	Υ_D	omitted?
ϕ	0	0.20	0.020	0.21	0.21	1.13	-6.78	-0.14	no
a	0	2.00	0.200	1.94	0.16	1.09	0.66	-0.10	no
b	0	2.00	0.200	1.97	0.04	1.02	0.31	-0.03	no
S_{wr}	0	0.20	0.020	0.21	0.25	1.16	-11.27	0.13	no
S_{or}	0	0.20	0.020	0.21	0.25	1.15	-11.15	0.14	no
K_{wm}	0	0.60	0.060	0.60	0.00	1.00	-0.32	0.01	no
K_{om}	0	0.60	0.060	0.60	0.01	1.00	0.46	-0.02	no
K	0	1.00	0.500	1.22	0.09	1.05	-0.19	-0.01	no

Table 23: Physical problem as in Table 3. E[**X**] equals p_i^{ref} in Table 3, and $\delta_i = 0.1$ for all variables, except for K which has a coefficient of variation equal to 1/2. Correlations as in Table 17. $\beta = 0.78$, $\Pr\{T \leq T_{0.80}\} = \Pr\{T \leq 1119\} = 0.22$, 4 iterations. This table is to be compared to Table 21.

	X correlated		**X** uncorrelated	
	$\omega = 0.5$	$\omega = 2.0$	$\omega = 0.5$	$\omega = 2.0$
ϕ	0.22	0.16	0.41	0.32
a	0.50	0.36	0.26	0.15
b	0.03	0.07	0.00	0.00
S_{wr}	0.10	0.16	0.06	0.10
S_{or}	0.09	0.12	0.04	0.05
K_{wm}	0.06	0.11	0.10	0.15
K_{om}	0.00	0.00	0.00	0.01
K	0.01	0.02	0.13	0.23

Table 24: Variations of α_i^2 with ω. The figures represent the extreme values of α_i^2 when $\omega \in [0.5, 2]$.

Although the tables themselves summarize the most interesting results from the sensitivity analysis, we make some general remarks and conclusions here.

- Water flooding versus polymer flooding gave very small differences in the results contained in the tables. Some differences between the computed probabilities did however exist. Similarly, negligible differences arose when treating all basic variables as normally distributed, except for a slight change in $\Pr\{T \leq T_\omega\}$. This means that in a stochastic analysis the presence of polymer or the choice between normal and lognormal distribution is not significant if the interest is to compute sensitivity measures.

- The influence of δ_i on the α_i^2 coefficients is negligible as long as δ_i is the same for all variables. Increasing δ_i for e.g. K only is reflected in a larger value of the importance factor α_i^2, especially if the variables are uncorrelated. It can be seen that δ_i has a significant influence on the computed probabilities. As expected, decreasing δ_i leads to greater sensitivity to $E[\mathbf{X}]$.

- When the basic variables are uncorrelated it is seen from the α_i^2 values that ϕ is the most important parameter. Also a and K contribute significantly. A ranking of the importance will be qualitatively the same as in the deterministic case, as long as δ_i is the approximately the same for all variables. In practice the coefficient of variation of K may be larger than for the other variables, and in this case K is by far the most important basic variable.

- With fairly correlated variables the situation is different: a is clearly most important while e.g. K plays a minor role. The importance measure of ϕ is more than halved compared to the uncorrelated case. Correlations have a significant impact on the relative importance of the stochastic variables.

- The stochastic analysis provide two different measures of input parameter importance:

  1. the importance factor α_i^2 which reflects the importance of modeling a parameter stochastically, and

  2. the Υ_E and Υ_D values which give information about the parameters that are most important to measure accurately in laboratory experiments.

The tables show that although a gives the largest contribution to the computation of $\Pr\{T \leq T_\omega\}$, the most important quantities to measure accurately is the expectation of the residual saturations and porosity, especially S_{wr}. The sensitivity to expectations is also much larger than the sensitivity to standard deviations.

41

- The presented tables correspond to computations where $\omega = 0.8$. It is of interest to investigate the sensitivity of our conclusions to variations in ω. The problems treated in Tables 16 and 17 have been run with different ω values. It turned out that α_i^2 varied monotonically with ω. Table 24 displays the extreme values of α_i^2 when $\omega \in [0.5, 2]$. It is seen that the internal ranking of the basic variables, according to the importance factor α_i^2, is not affected. Similar investigations of Υ_E and Υ_D showed that the variation with ω was not significant. As $\omega \to 1$ (from both sides) Υ_E increased in absolute value for all basic variables. The variation of Υ_D with ω did not exhibit a regular pattern common to all X_i's.

4.3.2 Heterogeneous reservoir

We now treat the problem in section 3.3.2 stochastically. We choose the input parameters at the midpoint $y_1 = \frac{1}{2}L$ as basic variables, again with exception of ξ and η. The distributions are as in the previous section.

Tables 25 and 26 present results with and without correlation between the basic variables, respectively. The physical problem corresponds to that treated in Table 13 (the aqueous phase is the most mobile phase at $x = 0$). In Table 29 we can see the effect of omitting stochastic variables after the first iteration. Linear space variation of parameters are employed in all tables, except in Table 28 where the variation is piecewise discontinuous as depicted in Figure 4. Table 30 corresponds to the physical problem in Table 15 (the aqueous phase is the less mobile phase at $x = 0$). Sensitivity to some deterministic parameters that enter the limit state function are shown in Tables 27 and 31. Similar sensitivity measures Υ_R have been calculated also corresponding to Table 25 and 28. However, the Υ_R values for the latter two cases were in qualitative agreement with those in Table 27. With a discontinuous space variation of p the $|\Upsilon_R|$ values were slightly larger than with a linear variation. The k value in the second column in all tables refers to the kth point in the coarse "parameter grid".

We see that most of the conclusions listed for the homogeneous case also holds here. There were small differences in the computed probabilities in the different tables. This indicates that a statistical analysis, where the interest is on the output probabilities, is robust. For example, no significant deviation due to linear or discontinuous space variation was observed, except that the discontinuous variation usually led to slower convergence of the search algorithm. Omission of basic variables where $\gamma_i \leq 1.03$ after the first iteration gave in general slower convergence (see e.g. Table 29) and inaccurate probability estimate.

parameter	k	E[X]	D[X]	x^*	α_i^2	γ_i	Υ_E	Υ_D	omitted?
ϕ	1	0.20	0.200	0.13	0.22	1.13	0.70	−0.10	no
a	1	2.00	2.000	1.12	0.11	1.06	0.10	−0.04	no
b	1	2.00	2.000	1.44	0.00	1.00	−0.01	0.00	no
S_{wr}	1	0.20	0.200	0.18	0.12	1.07	−0.96	0.12	no
S_{or}	1	0.20	0.200	0.16	0.03	1.01	−0.50	0.07	no
K_{wm}	1	0.60	0.600	0.58	0.26	1.16	−0.40	0.07	no
K_{om}	1	0.60	0.600	0.41	0.00	1.00	0.05	−0.01	no
K	1	1.00	1.000	0.97	0.25	1.16	−0.23	0.04	no

Table 25: Physical problem as in Table 13. E[X] equals p_1^{ref} in Table 11, and $\delta_i = 1/3$ for all variables. Uncorrelated variables. Linear space variation of parameters. $\beta = 0.76$, $\Pr\{T \leq T_{0.80}\} = \Pr\{T \leq 1789\} = 0.22$, 2 iterations.

parameter	k	E[X]	D[X]	x^*	α_i^2	γ_i	Υ_E	Υ_D	omitted?
ϕ	1	0.20	0.200	0.16	0.08	1.04	0.41	−0.03	no
a	1	2.00	2.000	0.92	0.41	1.31	0.21	−0.08	no
b	1	2.00	2.000	1.21	0.05	1.03	0.07	−0.02	no
S_{wr}	1	0.20	0.200	0.23	0.18	1.10	−1.03	0.09	no
S_{or}	1	0.20	0.200	0.22	0.11	1.06	−0.82	0.08	no
K_{wm}	1	0.60	0.600	0.55	0.15	1.08	−0.32	0.06	no
K_{om}	1	0.60	0.600	0.40	0.01	1.00	0.09	−0.02	no
K	1	1.00	1.000	0.76	0.01	1.01	−0.06	0.02	no

Table 26: Physical problem as in Table 13. E[X] equals p_1^{ref} in Table 13, and $\delta_i = 1/3$ for all variables. $\varrho(\phi, a) = 0.1$, $\varrho(\phi, b) = 0.1$, $\varrho(\phi, S_{wr}) = -0.4$, $\varrho(\phi, S_{or}) = -0.4$, $\varrho(\phi, K_{wm}) = 0.1$, $\varrho(\phi, K_{om}) = 0.1$, $\varrho(\phi, K) = 0.8$. Linear space variation of parameters. $\beta = 0.76$, $\Pr\{T \leq T_{0.80}\} = \Pr\{T \leq 1789\} = 0.22$, 4 iterations.

parameter	k	p_i^{ref}	Υ_R
ϕ	1	0.10	0.00
ϕ	3	0.30	0.89
a	1	1.00	0.05
a	3	3.00	0.08
b	1	3.00	0.01
b	3	1.00	-0.03
S_{wr}	1	0.10	-0.31
S_{wr}	3	0.30	-0.37
S_{or}	1	0.30	-0.12
S_{or}	3	0.10	-0.38
K_{wm}	1	0.90	-0.15
K_{wm}	3	0.30	-0.16
K_{om}	1	0.30	-0.02
K_{om}	3	0.90	0.06
K	1	0.50	-0.19
K	3	1.50	-0.03
ξ	1	0.10	-0.14
ξ	2	0.20	-0.11
ξ	3	0.30	0.00
η	1	1.50	0.01
η	2	1.00	0.01
η	3	0.50	0.00

Table 27: Sensitivity to well values. This table corresponds to Table 26.

parameter	k	$E[X]$	$D[X]$	x^*	α_i^2	γ_i	Υ_E	Υ_D	omitted?
ϕ	1	0.20	0.200	0.20	0.00	1.00	0.04	0.00	no
a	1	2.00	2.000	0.87	0.53	1.46	0.24	-0.09	no
b	1	2.00	2.000	1.25	0.04	1.02	0.05	-0.02	no
S_{wr}	1	0.20	0.200	0.22	0.19	1.11	-1.03	0.10	no
S_{or}	1	0.20	0.200	0.20	0.08	1.05	-0.73	0.08	no
K_{wm}	1	0.60	0.600	0.56	0.14	1.08	-0.29	0.05	no
K_{om}	1	0.60	0.600	0.40	0.01	1.01	0.10	-0.02	no
K	1	1.00	1.000	0.87	0.01	1.01	-0.05	0.01	no

Table 28: Physical problem as in Table 12. $E[X]$ equals p_1^{ref} in Table 12, and $\delta_i = 1/3$ for all variables. Correlations as in Table 26. Discontinuous space variation of parameters. $\beta = 0.81$, $\Pr\{T \leq T_{0.80}\} = \Pr\{T \leq 1978\} = 0.21$, 7 iterations.

parameter	k	E[X]	D[X]	x*	α_i^2	γ_i	Υ_E	Υ_D	omitted?
ϕ	1	0.20	0.067	0.16	0.43	1.33	2.39	−0.27	no
a	1	2.00	0.667	1.60	0.22	1.13	0.23	−0.10	no
b	1	2.00	0.667	1.89	0.00	1.00	0.00	0.00	yes
S_{wr}	1	0.20	0.067	0.24	0.15	1.08	−1.93	0.01	no
S_{or}	1	0.20	0.067	0.19	0.00	1.00	0.00	0.00	yes
K_{wm}	1	0.60	0.200	0.65	0.20	1.12	−0.64	0.03	no
K_{om}	1	0.60	0.200	0.57	0.00	1.00	0.00	0.00	yes
K	1	1.00	0.333	0.95	0.00	1.00	0.00	0.00	yes

Table 29: Physical problem as in Table 13. E[X] equals p_1^{ref} in Table 13, and $\delta_i = 1/3$ for all variables. Correlations as in Table 26. All basic variables for which $\gamma_i \leq 1.03$ after the first iteration, are omitted from the stochastic analysis. Linear space variation of parameters. $\beta = 1.00$, $\Pr\{T \leq T_{0.80}\} = \Pr\{T \leq 1789\} = 0.16$, 10 iterations.

parameter	k	E[X]	D[X]	x*	α_i^2	γ_i	Υ_E	Υ_D	omitted?
ϕ	1	0.20	0.200	0.16	0.09	1.05	0.49	−0.04	no
a	1	2.00	2.000	0.91	0.68	1.76	0.30	−0.12	no
b	1	2.00	2.000	1.34	0.01	1.00	0.03	−0.01	no
S_{wr}	1	0.20	0.200	0.20	0.07	1.04	−0.78	0.08	no
S_{or}	1	0.20	0.200	0.20	0.08	1.04	−0.79	0.09	no
K_{wm}	1	0.60	0.600	0.46	0.02	1.01	−0.15	0.03	no
K_{om}	1	0.60	0.600	0.47	0.04	1.02	−0.20	0.04	no
K	1	1.00	1.000	0.71	0.01	1.01	−0.07	0.02	no

Table 30: Physical problem as in Table 15. E[X] equals p_1^{ref} in Table 15, and $\delta_i = 1/3$ for all variables. Correlations as in Table 26. $\beta = 0.63$, $\Pr\{T \leq T_{0.80}\} = \Pr\{T \leq 1325\} = 0.27$, 4 iterations.

parameter	k	p_i^{ref}	Υ_R
ϕ	1	0.30	0.97
ϕ	3	0.10	0.10
a	1	3.00	0.03
a	3	1.00	0.12
b	1	1.00	-0.04
b	3	3.00	-0.01
S_{wr}	1	0.30	-0.53
S_{wr}	3	0.10	0.02
S_{or}	1	0.10	-0.50
S_{or}	3	0.30	-0.02
K_{wm}	1	0.30	-0.21
K_{wm}	3	0.90	-0.02
K_{om}	1	0.90	0.01
K_{om}	3	0.30	-0.29
K	1	1.50	-0.07
K	3	0.50	-0.23
ξ	1	0.30	-0.06
ξ	2	0.20	-0.03
ξ	3	0.10	-0.01
η	1	0.50	-0.01
η	2	1.00	-0.01
η	3	1.50	-0.01

Table 31: Sensitivity to well values. This table corresponds to Table 30.

5 Conclusion and discussion

Deterministic and stochastic sensitivity analysis represent two basically different ways of handling uncertainties. In the deterministic approach one calculates the effect (on the output) of a controlled *hypothetical* perturbation in the input. A stochastic analysis is based on the statistical structure in fictitious or performed observations and therefore applies to a specific real–world problem. When discussing sensitivity *in general* for a mathematical model the deterministic analysis probably gives the easiest perception of the model's "sensitivity", i.e. which input quantities that are most important to measure accurately, and how much the output is affected due to a change in input. However, in a particular physical problem where experience or measurements of the input data exist, a stochastic treatment have the advantage of incorporating the statistical information on the uncertainties and their effect on the output. The *practical* use of "sensitivity" (i.e. "What is most important to measure?") in the stochastic context is the sensitivity to statistical distribution parameters (Υ_E, Υ_D), and not sensitivity to the input quantities that are modeled as stochastic variables (α_i^2). The α_i^2 quantities gives valuable information about the input quantities that need to be modeled stochastically.

In this paper we have tried to determine the relative importance of some input parameters that enter a reservoir flow model. Polymer flooding including adsorption effects represented the simulated recovery process. For comparison we have also presented results from pure water flooding. The effect of including a polymer component in the injected phase showed to be significant in the deterministic sensitivity study, but not in the stochastic approach.

The deterministic sensitivity analysis was carried out by perturbing some input parameters and then measuring the effect on the time T to water breakthrough in the production well. Besides being of practical importance itself, T is also closely related to the total volume of oil produced until breakthrough. The input parameters studied herein were porosity, absolute permeability, quantities defining relative permeability curves and adsorption function parameters. The influence of the latter type of parameters was almost negligible. However, complete omission of the adsorption function had some effect on T (typically 20% in this study). Absolute permeability, porosity, and the exponent a in the relative permeability curve for the aqueous phase were the most important parameters. As the injected polymer concentration increased, or when the viscosity of the water/polymer mixture increased, the maximum relative permeability of the aqueous phase also became a significant parameter. The relative oil permeability seemed to be considerably less important than the relative water/polymer permeability. The sensitivity of T to perturbations in a was largest when a was small. In situations of greatest physical

47

relevance this means that the sensitivity is largest when the curve is linear.

One of the most serious deficiencies of a deterministic study is the problems with incorporation of the experimentally reported degree of functional relationship between the input parameters. A stochastic analysis of the present problem, based on a first order reliability method (FORM), showed that correlation between the stochastic variables had a significant effect on their relative importance. A striking feature was that the absolute permeability played a less important role in the stochastic analysis than in the deterministic one. However, in practice the coefficient of variation of the absolute permeability K may be larger than the coefficients of the other basic variables and then the importance of K increases, especially in the uncorrelated case. The expectations of the residual saturation variables, and occasionally also the porosity, showed to be the most important input data to a stochastic simulator. The output probabilities for T show little sensitivity to the type and dispersion of the distribution functions for the basic variables.

It is a general problem that the iterative procedure used in the stochastic analysis requires a large number of calls to the solution module for the partial differential equations. When applying this type of methods to problems in two and three space dimensions, the present approach is probably too CPU–time consuming, especially in heterogeneous problems. One way of reducing the work is to examine the importance factors after the first iteration and then omit unimportant basic variables from the rest of the analysis. This strategy has been tested, but not found particularly attractive. To prevent loss in probability accuracy, only a couple of the variables could be omitted. Sometimes omission led to slower convergence and thus no overall gain in efficiency. Simplified FORM methods, such as advanced mean–value FORM [4], should be tested.

The main conclusion from the deterministic analysis is that there are serious uncertainties in the output of a reservoir simulator, first of all due to missing information about the water/polymer relative permeability curve. The imposed space variation of the parameters, this will usually be piecewise linear or piecewise discontinuous variation on a very coarse grid, have a significant influence on the output results. The uncertainty in this type of models defines a level of accuracy which may be utilized when constructing an using solution methods for the partial differential equations. For example, tolerances in termination criteria used in simulators can be chosen large, and thereby increasing the efficiency. Another consequence could be that rather crude mathematical approximations to the governing equations, especially in more complicated black-oil or compositional models, may result in significant simplifications without loss in overall accuracy as long as the most important physical effects are maintained. One may then take advantage of these simplifications when constructing numerical methods. Rough approximations of the fractional flow curve used in front trackers [5] is an example

of a first step in this direction.

References

[1] M. B. Allen III, G. A. Behie and J. A. Trangenstein: Multiphase flow in porous media. *Lecture notes in engineering, Springer-Verlag*, 1988

[2] Aziz and Settari: Petroleum reservoir simulation. *Applied Science Publishers, London* 1979.

[3] N .A. Berruin and R. A. Morse: Waterflood Performance of Heterogeneous Systems. *SPE J.*, 829-836 (1979)

[4] P. Bjerager: Probability Computation Methods in Structural and Mechanical Reliability. *in W. K. Liu and T. Belytschko, eds.: Computational Mechanics of Probabilistic and Reliability Analysis*, Elme Press Int., Switzerland, 1989

[5] K. Bratvedt, F. Bratvedt, C. Buchholz, L. Holden, H. Holden and N. H. Risebro: A New Front-Tracking Method for Reservoir Simulation. *in proceedings: 64th Annual Technical Conf. and Exhibition of the SPE, Texas*, SPE 19805, 1989

[6] L. Y. Ding, R . K. Mehra and J. K. Donnelly: Stochastic Modeling in Reservoir Simulation. in proceedings: *10th SPE Symposium on Reservoir Simulation, Texas*, 303-320 (1989)

[7] A. I. Evrenos and A. G. Comer: Sensitivity Studies of Gas-Water Relative Permeability and Capillarity in Reservoir Modeling. *SPE paper 2668* (1969)

[8] R. E. Ewing: Problems arising in the modeling of processes for hydrocarbon recovery. *in R. E. Ewing (ed.): The Mathematics of Reservoir Simulation, SIAM*, 1983

[9] J. D. Huppler: Numerical Investigation of the Effects of Core Heterogeneities on Waterflood Relative Permeabilities. *SPE J.*, 381-392 (1970)

[10] T. Johansen, A. Tveito and R. Winther: A Riemann solver for a two-phase multicomponent process. *SIAM J. Sci. Stat. Comp.* (1989)

[11] A. Der Kiureghian and P-L. Liu: Structural reliability under incomplete probability information. *J. Eng. Mech., ASCE*, **112**, 85–104 (1986)

[12] A. Der Kiureghian and Jyh-Bin Ke: The stochastic finite element method in structural reliability. *Prob. Eng. Mech.*, **3**, 83–91 (1988)

[13] H. O. Madsen, S. Krenk and N. C. Lind: *Methods of Structural Safety*, Prentice-Hall, 1986.

[14] D. Peaceman: Fundamentals of numerical reservoir simulation. *Elsevier Scientific Publishing Company, Amsterdam*, 1977

[15] A. Selvig: Feasibility Study of Possible Applications of PROBAN in Reservoir Simulation. *Technical Report, A.S. Veritas Research*, 1988

[16] P. M. Sigmund and F. G. McCaffery: An Improved Unsteady-State Procedure for Determining the Relative-Permeability Characteristics of Heterogeneous Porous Media. *SPE J.*, 15-23 (1979)

[17] M. A. Yukler: Analysis of error in groundwater modelling. *Ph.D. thesis, University of Kansas*, 1976